# Multi-Scale Flood Simulations Under Climate Change Scenarios

Siavash Pouryousefi Markhali[1], Annie Poulin[2], and Marie-Amélie Boucher[3]

[1]École de Technologie Supérieure
[2]École de technologie supérieure, Université du Québec
[3]Université de Sherbrooke

January 3, 2023

**Abstract**

The present study focuses on quantifying the impact of the choice of spatio-temporal resolution and hydrology models on the projection of extreme flow and their link to the catchment size. We use two process-based distributed hydrology models forced with a large-ensemble regional climate model (50-member ClimEx dataset) over the 1990-2100 period at different spatio-temporal scales. The extreme summer-fall flow corresponding with each spatio-temporal resolution was extracted by pooling the members together and computing the empirical cumulative distribution function. The results show that by refining the time-step from daily to sub-daily, the summer-fall extreme flow projected over the future period exceeds that of the reference period for the small but not large catchments. By increasing the catchment size, the hydrology model's contribution to the variability of extreme flow increases. Moreover, the choice of spatial resolution affects the extreme flow's trend in terms of magnitude, significance, and direction. But no pattern regarding the catchment size and spatial discretization variations exists.

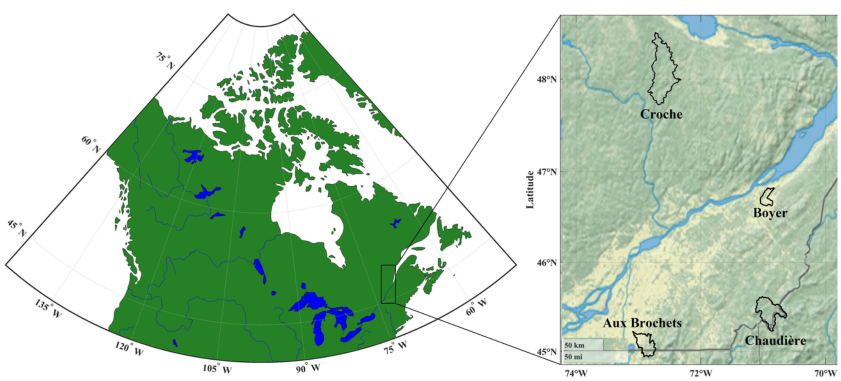

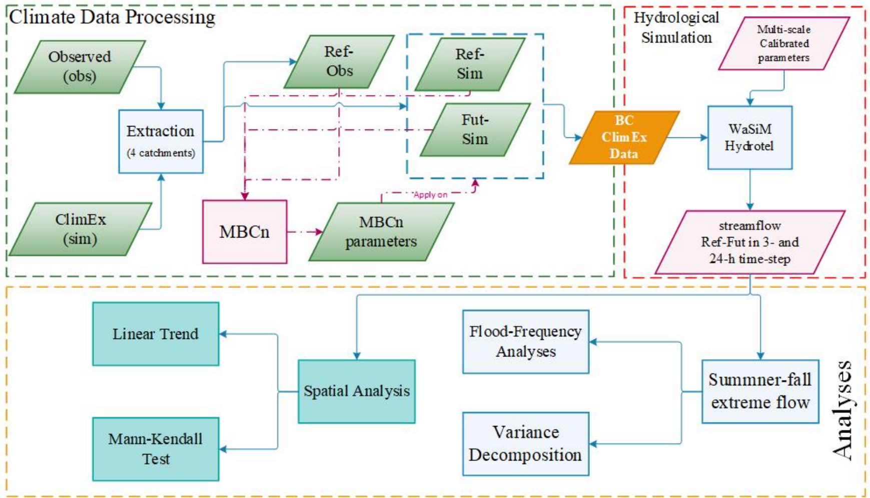
Climate Data Processing
Observed (obs)
Extraction (4 catchments)
ClimEx (sim)
Ref-Obs
Ref-Sim
Fut-Sim
MBCn
MBCn parameters
Apply on
BC ClimEx Data
Hydrological Simulation
Multi-scale Calibrated parameters
WaSiM Hydrotel
streamflow Ref-Fut in 3- and 24-h time-step
Analyses
Linear Trend
Spatial Analysis
Mann-Kendall Test
Flood-Frequency Analyses
Summner-fall extreme flow
Variance Decomposition

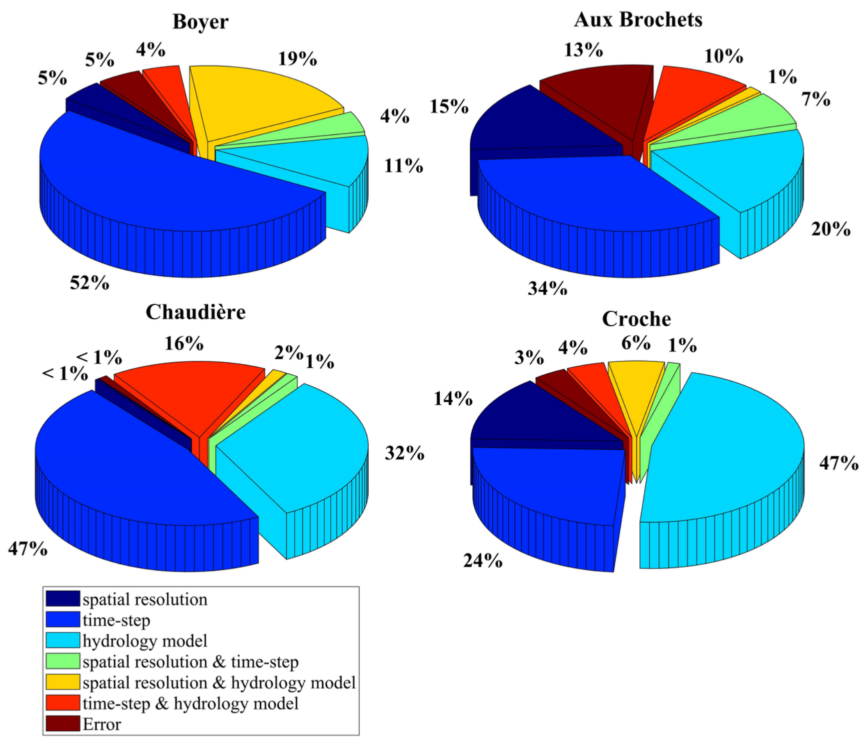
Boyer
5%
5%
4%
19%
4%
11%
52%
Aux Brochets
15%
13%
10%
1%
7%
20%
34%
Chaudière
< 1%
< 1%
16%
2%
1%
32%
47%
Croche
14%
3%
4%
6%
1%
47%
24%
spatial resolution
time-step
hydrology model
spatial resolution & time-step
spatial resolution & hydrology model
time-step & hydrology model
Error

# Multi-Scale Flood Simulations Under Climate Change Scenarios

**S. P. Markhali[1], A. Poulin[1], and M. A. Boucher[2]**

[1]Department of Construction Engineering, École de technologie supérieure, Montreal, Canada
[2]Civil and Building Engineering Department, Université de Sherbrooke, Sherbrooke, Canada

**Key Points:**

- Refining the time-step of the modeling results in higher summer-fall flood magnitudes in the future for the small but not large catchments.
- Variation of spatial resolution changes the trend's magnitude, and/or direction and/or significance.
- By increasing the catchment size, the contribution of the hydrology model in the variability of flood projection increases.

Corresponding author: S. P. Markhali, siavash.pouryousefi-markhali.1@ens.etsmtl.ca

## Abstract

The present study focuses on quantifying the impact of the choice of spatio-temporal resolution and hydrology models on the projection of extreme flow and their link to the catchment size. We use two process-based distributed hydrology models forced with a large-ensemble regional climate model (50-member ClimEx dataset) over the 1990-2100 period at different spatio-temporal scales. The extreme summer-fall flow corresponding with each spatio-temporal resolution was extracted by pooling the members together and computing the empirical cumulative distribution function. The results show that by refining the time-step from daily to sub-daily, the summer-fall extreme flow projected over the future period exceeds that of the reference period for the small but not large catchments. By increasing the catchment size, the hydrology model's contribution to the variability of extreme flow increases. Moreover, the choice of spatial resolution affects the extreme flow's trend in terms of magnitude, significance, and direction. But no pattern regarding the catchment size and spatial discretization variations exists.

## 1 Introduction

Flood hazard continues to threaten human life and inflict costs on infrastructures and urban areas, as multiple devastating events have been reported in recent years around the world (Merz et al., 2021). Accurate flood estimation remains a critical issue and the traditional stationary assumption employed by flood estimation methods, whether empirical or process-based, fails to account for changing climate signal, leading to inaccurate estimations of exceeding probability of peak flow (Blöschl et al., 2013; François et al., 2019; Montanari & Koutsoyiannis, 2014). Moreover, a lack of knowledge regarding flood-generating processes at different scales with complex and non-linear catchment responses in space and time complicates the estimation of flood return period using process-based hydrology models (K. Beven, 2019; Blöschl, 2022b). The present research aims to investigate how the discrete representation of catchments in process-based distributed hydrology models can affect flood projection under climate change scenarios. The study is conducted for snow-dominated Nordic catchments located in Canada.

Global warming is expected to increase the magnitude and frequency of extreme precipitation across different parts of the world (Min et al., 2011; Westra et al., 2013; Alexander et al., 2006; M. Donat et al., 2013; Field et al., 2012; Masson-Delmotte et al., 2021; Fowler et al., 2021; Martel et al., 2021). This projected increase can be attributed to the increase of water holding capacity of the atmosphere: Based on Clausius–Clapeyron rate, the water holding capacity of atmosphere increases by 7% per 1° increase of temperature (Molnar et al., 2015; Westra et al., 2014). This however cannot directly be translated into precipitation, as the amount of available humidity required for precipitation complicates the relationship (Lochbihler et al., 2017; Yin et al., 2018). Depending on moisture availability, warming can cause intensification of convective storms with daily or subdaily scales (Westra et al., 2014).

Considering that precipitation is an essential driver of flood events, different reactions from small and large-scale catchments should be expected: for small catchments, the response time is short and the maximum flow peak can be deduced from a storm with a duration equal to the longest flow path in the catchment (Blöschl, 2022a). Given that the short period of convective rainfall matches the residence time of small catchments, these catchments are the most vulnerable to flooding from convective rainfall, which is expected to increase due to climate change (Viglione & Blöschl, 2009; Viglione et al., 2016; Breinl et al., 2021). Regarding large catchments of more than a thousand square kilometers, it is unlikely that a convective storm leads to a flooding event considering the larger storage capacity and longer travel time (Contractor et al., 2021). For Nordic snow-dominated catchments, since global warming will likely reduce the amount of snow that accumulates, the magnitude of the spring freshet is expected to diminish. However, even for those catchments, it is anticipated that the frequency and magnitude of convection-driven summer-fall floods, to which small catchments are sensitive, will increase (M. G. Donat et al., 2016).

High temporal resolution time series (hourly) of historical data to evaluate the trend of convective storms and consequent floods are difficult to find. A common practice is therefore to use a climate modeling chain and perform simulations at high spatio-temporal resolutions (e.g., Swain et al., 2020; Do et al., 2020). Regional Climate Models (RCMs) offer such high-resolution time series at a local scale (Mearns et al., 2017; Leduc et al., 2019). Moreover, the incorporation of convective parameterization has enhanced their capability to capture convective storms (Kendon et al., 2017; Prein et al., 2015; Mooney et al., 2017). More recently, large-ensemble RCM datasets have received attention (Martel, Mailhot, & Brissette, 2020; Sanderson et al., 2018; Aalbers et al., 2018). Large-ensembles are generated by running RCMs several times, each time with slightly different initial conditions (Deser, Knutti, et al., 2012; Deser, Phillips, et al., 2012). Multiple values are calculated per time-step, which eliminates the need to fit a parametric distribution on the dataset to compute extreme flows (Martel, Mailhot, & Brissette, 2020; Faghih et al., 2022).

Hydrology models are the last component of a hydro-climate modeling chain (Sidle, 2021). Proportional to the growth of computational power, process-based hydrology models are increasingly used for impact studies (Zhang et al., 2018; Dembélé et al., 2020; Pandey et al., 2019; Duethmann et al., 2020; Zhong et al., 2018). These models solve the governing equations of hydrological processes (with varying degrees of simplification) per grid cell. Distributed models further use routing algorithms to direct accumulated water towards neighboring cells until the basin outlet (Clark et al., 2015, 2017). The advantage of using distributed physics-based hydrology models is to represent the topography, land use, and soil structure in the model, to obtain a detailed distribution of hydrological variables inside the catchment (Refsgaard, 1995). Therefore, these models are useful to study the internal dynamics of state and flux variables (Golden & Knightes, 2011; Gebremicael et al., 2019; Sidle et al., 2017).

scale issue is the subject of a long ongoing debate in the scientific community (Blöschl & Sivapalan, 1995; Blöschl et al., 2019). Despite numerous types of research to understand runoff generation processes, there are still unknowns about upscaling from profile scale (1m) to catchment scale and beyond. For example, while the infiltration excess is the governing process at profile-scale (Horton, 1933), the spatial connectivity of hydrological processes has a central contribution in runoff generation at the hillslope scale (Dunne & Black, 1970; Noguchi et al., 1999; Sidle, 2006). Moreover, the contribution of overland connectivity in flow generation and sediment transport and their feedback loop add to the non-linearity of runoff generation (Gomi et al., 2002; Jencso et al., 2010; López-Vicente et al., 2017; Koci et al., 2020). The non-linearity from hillslope- to catchment scale is also significant, as the traditional bottom-up Freeze and Harlan (1969) approach to linearly combine all hillslopes so as to compute catchment response has been challenged. Dooge (1986), for example, suggests that a catchment is an "organized complex system", in the sense that the development of co-evolutionary surface and subsurface patterns contributes to catchment drainage and runoff generation (Sivapalan & Blöschl, 2015; Savenije & Hrachowitz, 2017). Adapting the bottom-up approach to these criticisms, there were efforts to combine the hillslope's responses by considering the spatio-temporal covariance of hydro-climate variables for flood simulations (Woods & Sivapalan, 1999; Viglione et al., 2010).

The spatio-temporal discretization of distributed models can potentially modify land-use and soil structures and result in variations of hydraulic conductivity as well as surface and subsurface hydrological connectivity (K. J. Beven, 2000). This can potentially lead to variations in the peak flow or seasonal flow. Many studies have explored the effect of land-use change on streamflow (Singh et al., 2015; Li et al., 2019; Yang et al., 2019;

Tavangar et al., 2019). Using more than one land use scenario is a common approach to studying land use change impacts (Breuer et al., 2009; Huisman et al., 2009; Viney et al., 2009; Bormann et al., 2009). The results show that land use change can increase/decrease the peak flow, depending on catchment size and/or soil structure. Conversely, paired catchment studies have demonstrated that land-use changes can modify mean seasonal streamflow but has minor effects on the peak flow (Brown et al., 2005). The effects of spatio-temporal discretization using process-based models have rarely been investigated for natural catchments. Most previous studies concentrated on urban catchments, with a high degree of impermeability and small size (e.g. Cao et al., 2020; Krebs et al., 2014; Zhou et al., 2017; Cao et al., 2020). In this context, multiple studies have shown that variation of spatio-temporal resolution can reorient flow direction and significantly change the flow peak (Zhou et al., 2017; Ichiba et al., 2018; Warsta et al., 2017).

Markhali et al. (2022) have shown that the spatio-temporal discretization of a catchment in a model can affect the representation of surface and subsurface hydrological processes in that model and generate a significant variation in the distribution of hydrological variables including streamflow. Such variations are most important in flat catchments or catchments with considerable human intervention (i.e., agricultural lands). The present study focuses on extreme summer-fall flow using a hydro-climate modeling chain. A range of catchments with different surface areas (from below 200 $km^2$ to more than 1500 $km^2$) are selected to facilitate the investigation of the combined impacts of climate change and the spatio-temporal discretization in the hydrological model. More specifically, we intend to verify the following hypotheses for the catchments at hand:

- By refining the time step of projection, the small catchments see a larger increase in the magnitude of summer-fall floods than the large catchments.
- The change in the spatio-temporal scale of modeling causes variability in the projection of extreme flow. By increasing the catchment size, the contribution of hydrology model and spatial scale in that variability increases, and that of the time-scale decreases.

The hypotheses will be examined by forcing two process-based distributed models with large-ensemble simulated climate data. To examine the impact of spatio-temporal discretization, the simulations will be performed at different spatial (100, 250, 500, 1000 $m$) and temporal scales (3- and 24-hour time-steps). The structure of this research is as follows: Section 2 provides a detailed explanation of the study area, available data, bias correction method, hydrology models, and the experimental plan. Section 3 presents the results of the experiments, which are discussed in Section 4. Section 5 provides concluding remarks and a suggestion for future works.

# 2 Method and Data

## 2.1 Study Area

The study area includes four catchments located in southern Quebec, Canada (Figure 1). These catchments range from less than 200 $km^2$ to more than 1500 $km^2$ and were selected from diverse land use and hydrological regions. This helps evaluate catchment responses under climate change based on their size and other characteristics, such as land-use and topography. Table 1 briefly describes catchments' characteristics.

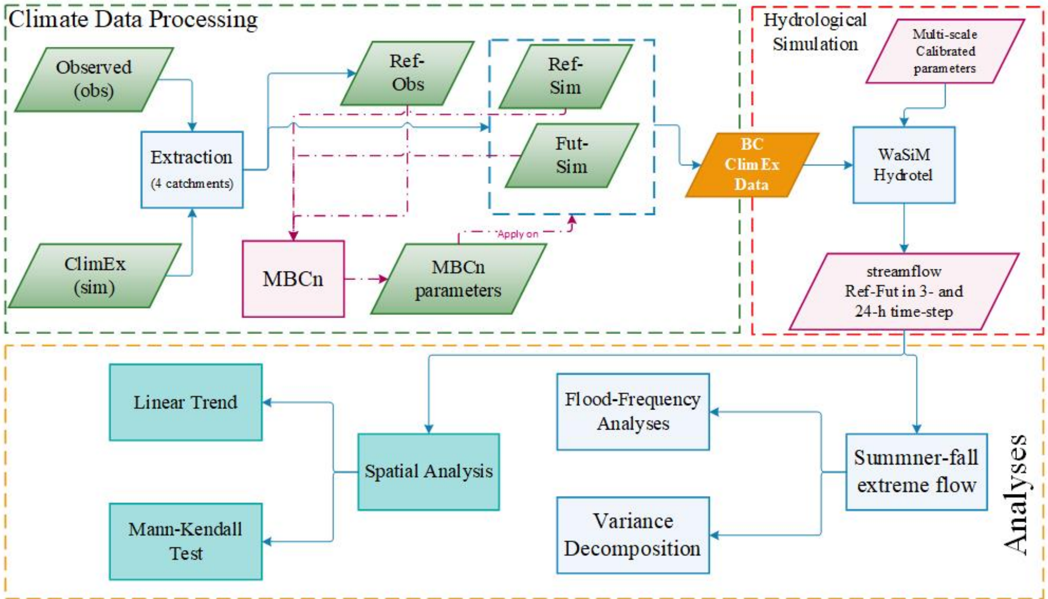


**Figure 1.** Location of the catchments used in this study

**Table 1.** Area and main hydro-climatic characteristics of the catchments used in this study

| Number | Name | Area($km^2$) | precipitation($mm/yr$) | streamflow ($m^3/s$) | temperature ($°C$) |
|---|---|---|---|---|---|
| 050135 | Croche | 1563 | 1139.36 | 30.70 | 2.74 |
| 023427 | Chaudière | 781 | 1208.65 | 16.47 | 3.72 |
| 030424 | Aux Brochets | 584 | 1329.34 | 10.52 | 6.23 |
| 023004 | Boyer | 191 | 1396.76 | 4.45 | 4.15 |

### 2.2 Datasets

24- and 3-hour observed streamflow series were obtained from the Direction de l'Expertise Hydrique (DEH) of the Ministère de l'Environnement et de la Lutte contre les changements climatiques (MELCCC) for 2000-2017. Regarding meteorological data, we used the ERA5(ECMWF ReAnalysis5, Hersbach et al., 2020) gridded dataset to calibrate the hydrology models and simulate streamflow for the present-day climate. (Tarek et al., 2020) have shown that ERA5 provides an accurate representation of meteorological conditions for catchments located in North America. We also used the ClimEx large ensemble (Climate change and hydrological Extremes project, Leduc et al., 2019). ClimEx is a 50-member climate dataset, driven by dynamically downscaling the second version of the Canadian Earth System Model large ensemble (CanESM2-LE; Swart et al., 2019), using the 5th generation of the Canadian Regional Climate Model (CRCM5). The simulations are driven by the RCP 8.5 scenario for the period covering 1951-2100, with hourly time steps and an 11° spatial resolution.

### 2.3 Bias Correction

The MBCn (N-dimension multivariate bias correction) (Cannon, 2018) method was selected to bias correct precipitation and temperature time-series extracted from ClimEx. MBCn is an advanced quantile-mapping technique (Meyer et al., 2019; Cannon et al., 2020). The method transfers all characteristics of the distribution of observations to their simulated values according to the climate model. It maintains the trends of projections per quantile, which is essential to accurately assess the impact of climate change (Faghih et al., 2022).

### 2.4 Hydrological models

The following section introduces the hydrology models that are used in this study. Both models are distributed, process-based, and computationally intensive. However, they each have their own methods of representing hydrological processes, and their approaches to aggregate the catchment response are also different.

#### *2.4.1 WaSiM*

WaSiM (Water balance Simulation Model) operates on a raster system (Schulla & Jasper, 2007). The model's structure comprises multiple sub-models (e.g., infiltration, evapotranspiration, snow accumulation and melt, unsaturated zone, etc.) that run on each grid cell and time-step, providing the opportunity to use parallel computing. WaSiM offers two options for calculating the infiltration and percolation: the Topmodel approach, or Richard's equation. The first approach is a modified version of the conceptual model Topmodel, following K. Beven (1997). The second approach is more physically-based and is the one used in this study. All the sub-models that are selected for WaSiM are named in Table 2.

#### *2.4.2 Hydrotel*

Hydrotel is widely used in Quebec for research and operations (e.g., Martel, Brissette, & Poulin, 2020; Turcotte et al., 2020; Lucas-Picher et al., 2020). In Hydrotel, the catchment is divided into HRUs (Hydrological Response Units) that have similar soil and land-use characteristics. Sub-catchments are formed by aggregating HRUs. Hydrotel is compatible with GIS and remotely-sensed data (Fortin et al., 2001a). A mixture of physical, conceptual, and empirical relationships are used to represent the hydrological processes, which makes Hydrotel slightly less physics-based than WaSiM. For example, the vertical water balance and the representation of soil water content are computed through a sub-routine called BV3C (Bilan Vertical à 3 Couches), which divides the soil column into 3 layers and controls infiltration, interflow and baseflow, based on a semi-physical moisture accounting equation (Fortin et al., 2001a). Like WaSiM, Hydrotel provides multiple options for representing the hydrological processes of a catchment. Table 2 lists the submodels that are used in this study.

**Table 2.** The submodels used to represent the hydrological processes in Hydrotel and WaSiM.

| Submodels | Hydrotel | Wasim |
|---|---|---|
| Interpolation | Thiessen polygons | Thiessen polygons |
| Snow melt/accumulation | Degree-Day Method | Degree-Day Method |
| Potential evapotranspiration | Hydro-Quebec (Fortin et al., 2001b) | Hamon (Hamon, 1961) |
| Real evapotranspiration | BV3C | Richards' Eq. |
| Infiltration and percolation | BV3C | Richards' Eq. |
| Channel routing | Kinematic Wave Eq. | Kinematic Wave Eq. |

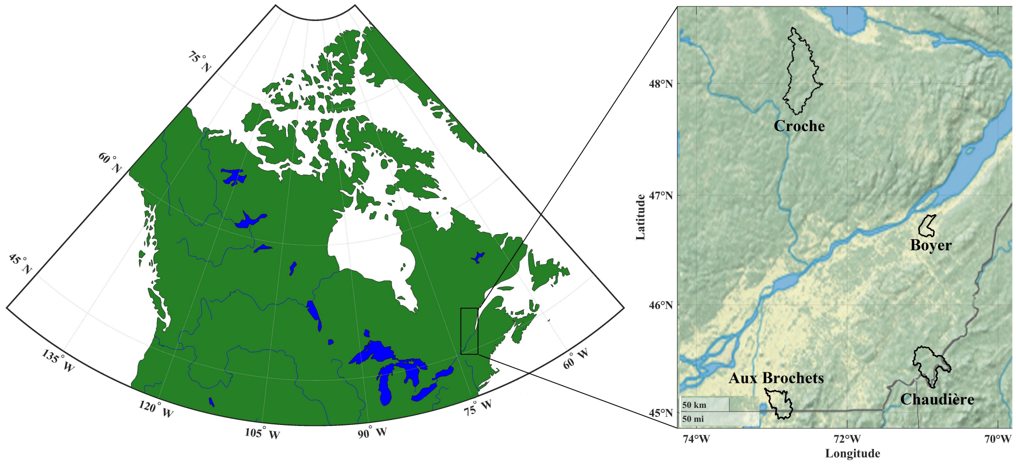


**Figure 2.** Schematic explanation of the experimental plan and methods.

### 2.5 Experimental plan

#### *2.5.1 Climate Data Processing*

Figure 2 shows the experimental plan for this study. The first panel on the top left, bounded by the green dashed line, shows the details regarding climate data processing. The first step is the extraction of the simulated and observed meteorological data (temperature and precipitation) for the selected catchments. The reference period for the observed dataset ($Ref{-}Obs$) spans from 1991 to 2010. ClimEx simulations are also split into reference ($Ref - Sim$) and future ($Fut - Sim$, 2011-2099) periods. In the next step, the 50-member ClimEx (i.e., $Ref{-}Sim$ and $Fut{-}Sim$) are pooled together into one long time series per period. This pooling helps to maintain the internal variability of the simulated climate data after bias correction. This is because individual bias correction of each member eliminates the spread of simulations and creates rather similar time series. While addressing internal variability is not among the objectives of this research, maintaining that helps accurate calculation of extreme flows (Faghih et al., 2022). The $Ref{-}Obs$ and $Ref{-}Sim$ datasets, which include precipitation and temperature for both the reference and future periods, are further received by MBCn to obtain correction factors based on multi-variate quantile mapping. A single set of correction factors was computed per calendar month and applied to the simulated climate data. The pooled bias-corrected datasets are reversed back to the 50-member time series, ready to use as the inputs of the hydrology models.

#### *2.5.2 Hydrological Simulation*

The Hydrology models are calibrated with four spatial (100, 250, 500, 1000 $m$) and two temporal resolutions (3- and 24-hour). The datasets are split into calibration and validation periods with equal duration. The Dynamically Dimensioned Search (DDS; Tolson & Shoemaker, 2007) with a 0.2 perturbation factor was employed to calibrate the models. The DDS technique scales the parameters search space according to a budget specified by the user. Given that both WaSiM and Hydrotel are computationally intensive, this is an advantage over other search methods. In addition, the efficiency of DDS with global parameter perturbations at the beginning and narrowing down the search space by the end of the process has been confirmed in the literature (e.g., Huot et al., 2019).

Based on the existing literature and following experts' recommendations as well as the team who develops and maintains WaSiM, 12 parameters were calibrated, including seven parameters that are involved with the unsaturated zone subroutine, two parameters linked to potential evapotranspiration, one parameter for snow accumulation and melt, and two parameters for spatial interpolation. The remaining parameters were left to their default values following the WaSiM documentation (Schulla & Jasper, 2007). Regarding Hydrotel, of 28 models' parameters, 11 have been calibrated and the others were left to their default values according to Hydrotel's user manual. Out of the 11 calibration parameters, three belong to vertical water balance, six to the snow accumulation and melt routine, and one to the infiltration and interpolation components (see Huot et al. (2019) for more details about the parameters).

The Kling-Gupta Efficiency criterion (KGE; Gupta et al., 2009) is the objective function for the calibration of both WaSim and Hydrotel. Compared to other criteria such as the Nash–Sutcliffe efficiency (NSE), the KGE is a better choice for snow-dominated catchments. This is because the observed mean is the baseline model for NSE and for the catchments with high seasonal variability, the measure tends to overestimate modeling skill (e.g., snowmelt streamflow)(Gupta et al., 2009). Equation 1 was used to calculate the KGE

$$KGE = \sqrt{(r-1)^2 + (\frac{\sigma_{sim}}{\sigma_{obs}} - 1)^2 + (\frac{\mu_{sim}}{\mu_{obs}} - 1)^2} \tag{1}$$

where $r$ is the linear correlation between observed and simulated streamflow values, $\sigma_{sim}$ is the standard deviation of the observations, $\sigma_{obs}$ is the standard deviation of the simulation, $\mu_{sim}$ is the simulation mean, and $\mu_{obs}$ is the observation mean.

After obtaining the parameters corresponding with the four spatial resolutions and two temporal resolutions mentioned above, climate simulations from ClimEX were used as inputs to the hydrology models for 1991 to 2100; as mentioned in the top right panel bounded with the red dashed border in Figure 2.

#### *2.5.3 Analyses*

The panel at the bottom of Figure 2, with a dashed orange border, shows the analyses and experiments that have been carried out to verify the two hypotheses which are the object of this research. To verify the first hypothesis, extreme summer-fall flows are calculated for different spatio-temporal simulations. The streamflow series were split into historical (1991-2010) and far-future periods (2081-2100) to estimate the change of extreme flow under climate change. A 50-member ensemble of simulated streamflows obtained from forcing hydrology models with CliMeX was pooled together to create a time series comprising 1000 years of data (20 years $\times$ 50 members). This very large ensemble was created to estimate projected yearly extreme flows without the need to fit a parametric distribution. The annual maximum summer-fall flows (July-November) is extracted from the data and an empirical cumulative distribution function is created for both periods (present-day and far future). This allows us to compare the distributions of projected extreme flows in the historical and far-future periods for different combinations of spatio-temporal discretizations (we have four spatial and two temporal resolution that amounts to 8 different combinations). The studied extreme flow values are based on the following percentiles : 50, 90, 95 and 99 (representing 2-, 10-, 20- and 100-year retur periods). The procedure regarding pooling and extracting the extreme values is the same as in Martel, Brissette, and Poulin (2020).

In order to verify the second hypothesis, we use variance decomposition (Montgomery, 2017) to find the contribution of different factors in the total variance of the projected extremes. Variance decomposition is a simple but robust and widely applied method (e.g. Addor et al., 2014; H. K. Meresa & Romanowicz, 2017; Wang et al., 2020; H. Meresa et al., 2022). Equation 2 shows the application of the method in this study,

$$\Delta U_{i,j,k} = H_i + S_j + T_k + H_i * S_j + H_i * T_k + S_i * T_k + \epsilon \quad (2)$$

where $\Delta U$ is the total variance of projected extreme flow, $H_i$, $S_j$, and $T_k$ are different choices of hydrology model, spatial resolution, and time-step, and $\epsilon$ represents a Gaussian white noise.

To quantify the change in the streamflow when the hydrology model's spatial resolution varies, annual maximum summer-fall flows were extracted per grid and the linear trends corresponding to those grids were computed for the entire 1991-2100 period. The linear trend analysis has frequently been used for quantifying the change in the climate variables (Barnes & Barnes, 2015; Zhuan et al., 2018; Ding & Steig, 2013). Note that the non-linear quadratic and cubic polynomials produced poor results for this case study. The widely used non-parametric Mann-Kendall trend test (Ali et al., 2019) was also applied to identify the trend at a 0.05 significance level. In this test, the null hypothesis ($H_0$) assumes no trend and the alternative hypothesis ($H_1$) assumes the existence of a trend at a 0.05 significance level.

# 3 Results

## 3.1 Annual Hydrographs

Figures 3 and 4 show the annual simulated hydrographs for the reference and future periods at 3- and 24-hour time-steps using WaSiM and Hydrotel for the Boyer and Croche catchments. These catchments are the smallest and largest, respectively. In these figures, the ensemble of streamflow simulations is based on the ClimEx dataset, for the 1990-2100 period with various spatial resolutions for both hydrology models ($100, 250, 500$, and $1000m$). The median of each ensemble is displayed as a solid line and the observed data is the dashed black line.

Figure 3, a) to d) show the WaSiM simulations with 3- and 24-hour time-steps for the Boyer catchment. The observed data is located inside the spread of simulations and the timing of the peaks is approximately the same for both the simulation and the observations (panels a and c). However, the simulation underestimates the magnitude of the median peak flow. We also want to assess how changing the spatial resolution would affect the simulation of low and high flows. According to Figure 3, a) to d), the simulation of low flows is more sensitive to variations in spatial scale than that of high flow. Moreover, this sensitivity also increases by refining the time-step from 24- to 3-hour. Figure 3 e) to f) shows Hydrotel simulations. As for WaSim, the observed value is located inside the ensemble's spread (panels e and g). Moreover, the ensemble's median is closer to the observation than that of WaSiM simulations. With Hydrotel, the simulation of high flows is more sensitive than the simulation of low flows to changes in spatial resolution, which is the opposite behavior of WaSim. Again, this sensitivity to the change of spatial resolution is higher for the 3-hour time-step than for the 24-hour time-step. Comparing future ( panels a, c, e, g) and reference (panels b, d, f, h) periods, a backward shift of the spring freshet from mid-April to mid-May with significantly lower amplitude can be seen, regardless of the time-step and spatial resolution, for both Hydrotel and WaSim. Overall, WaSiM shows higher sensitivity to changes in spatial resolution than Hydrotel, which is expected as the model is fully distributed and more physically representative in terms of the vertical water budget in the soil.

Figure 4 shows the result of the same exercise, but for the Croche catchment. Panels a) to d) show WaSiM simulations with 3- and 24-hour time steps. Compared to Figure 3 for the Boyer catchment, WaSiM (panels a and c) shows more skill, as the medians of all the simulations follow the observations closely. In general, varying the spatial resolution of the hydrology model has only minor effects on these simulations, except for the simulations with a 3-hour time-step. Hydrotel's simulations (panels e to h) show an

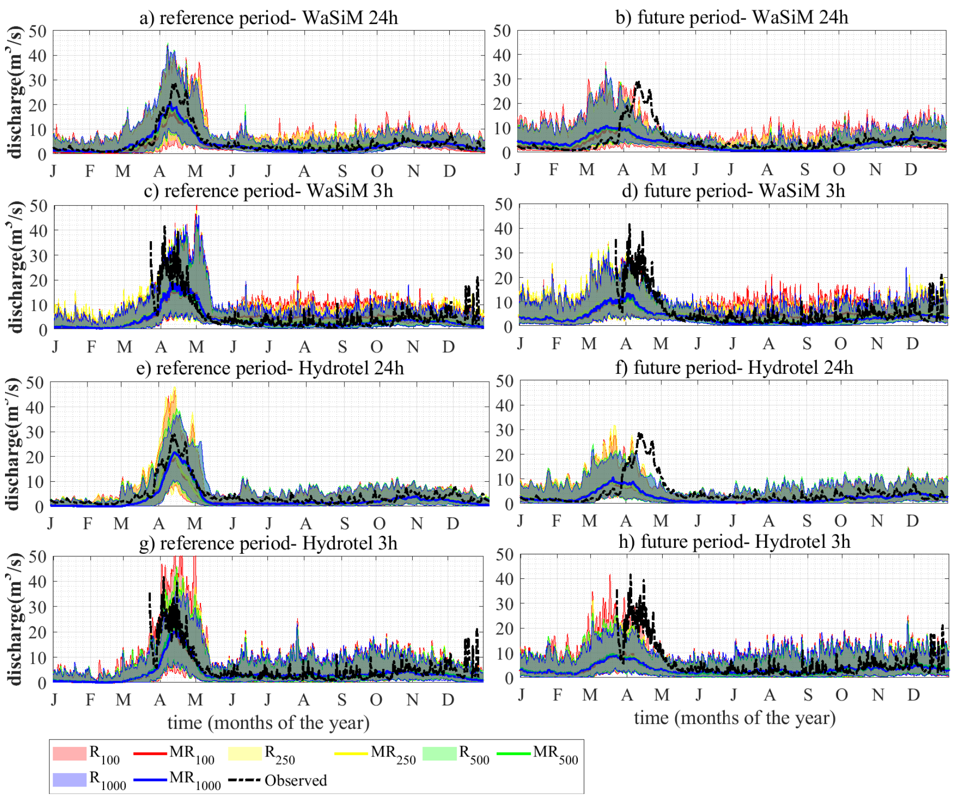


**Figure 3.** Ensemble of annual hydrographs forced by ClimEx dataset per resolution and compared with observed streamflow (dashed black line) for the Boyer catchment. R and the following number represents the spatial resolution in $m$ and MR with the following number represents the median of the ensemble.

underestimation of peak streamflow when the ensemble median is compared to the observations. This underestimation is larger for the simulations with a 24-hour time-step than for the 3-hour time-step. In terms of spatial resolution, both WaSim and Hydrotel are more sensitive to changing the spatial resolution when the time-step of the simulations is finer. Comparing the future and reference periods, a significant attenuation in the magnitude of the spring freshet and a backward shift in the timing of the peak can be observed for both models. There is also a considerable increase in streamflow in the fall and winter months (November to March) when comparing the present and future periods.

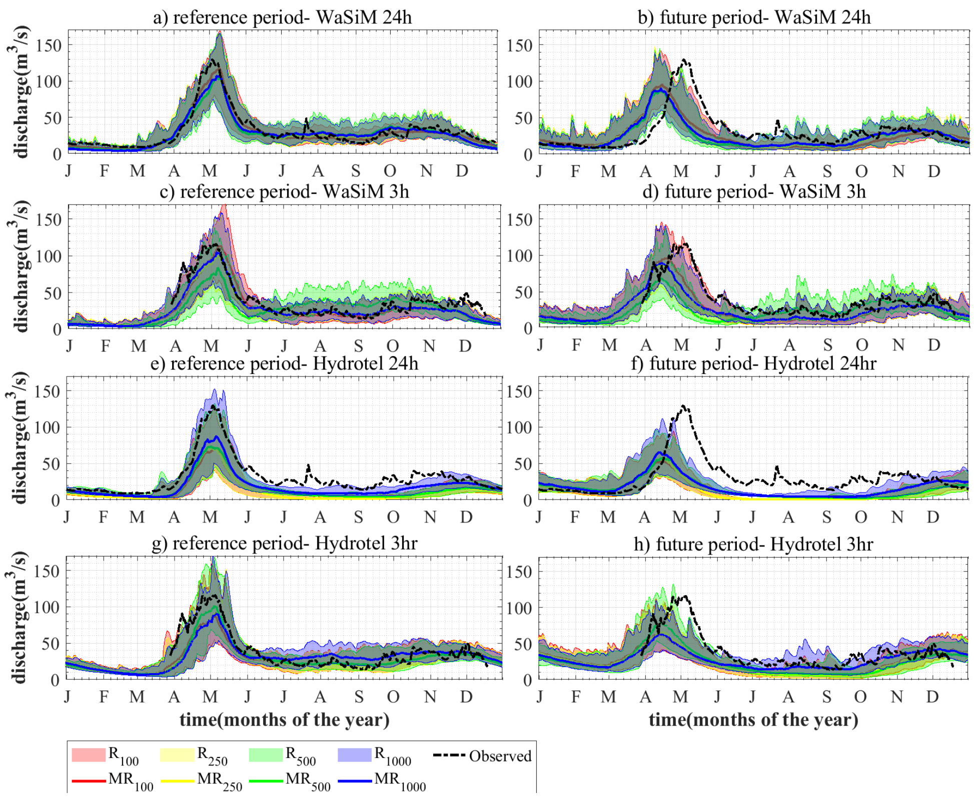


**Figure 4.** Ensemble of annual hydrographs forced by ClimEx dataset per resolution and compared with observed streamflow (dashed black line) for the Croche catchment. R and the following number represents the spatial resolution of simulations in $m$ and MR with the following number represents the median of that ensemble.

Overall, it is not clear from Figures 3 and 4, whether there exists a pattern regarding the interaction between catchment size and the choice of hydrology model and spatio-temporal resolution. However, each of these elements can distinctly alter the catchment responses.

### 3.2 Spatial distribution of the hydrological variables

Figure 5 shows the spatial distribution of actual evapotranspiration (AET) and snow depth (SD) for the Croche catchment. The figure shows that by the end of the century (period 2081-2100), AET will increase by 5 to 10 % according to Hydrotel simulations (panels a to d) and 15 to 30% according to WaSiM simulations (panels e to h). A significant negative change in snow depth is observable, as by the end of the century, the

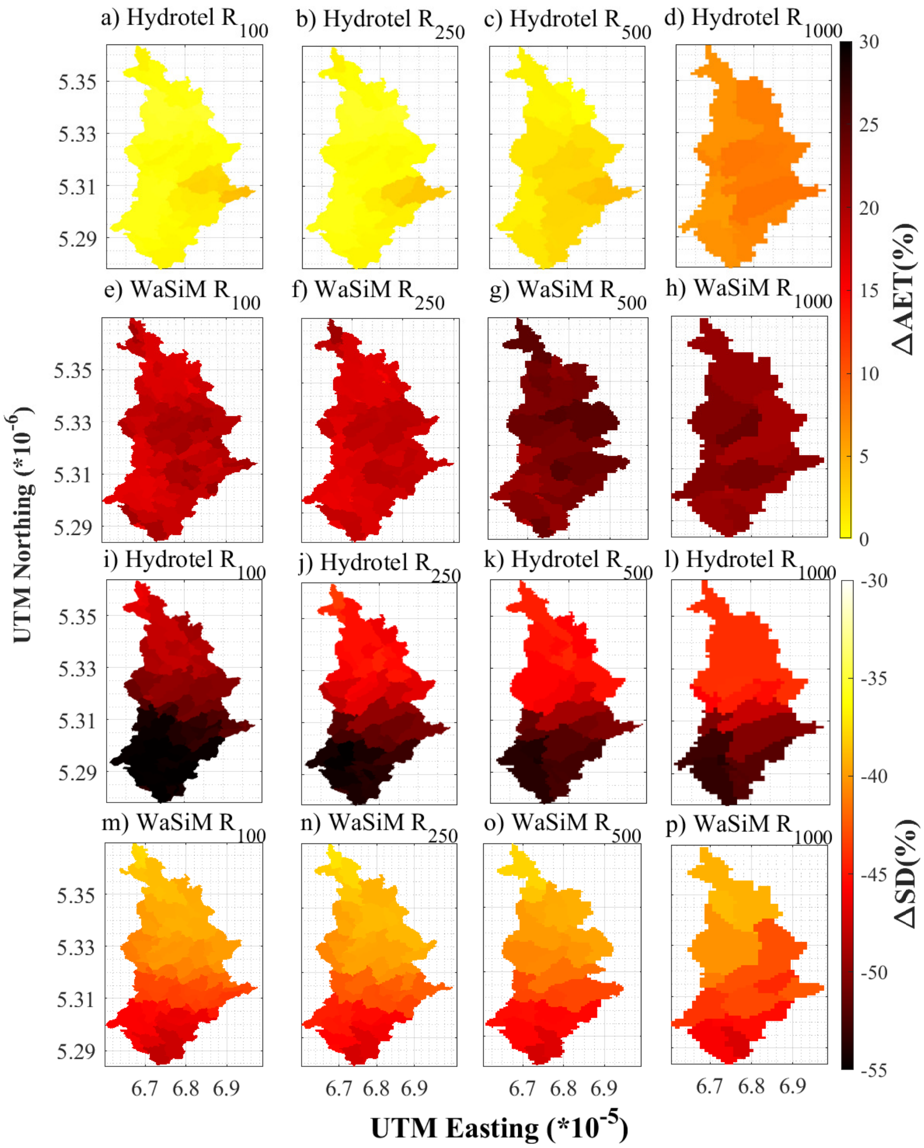


**Figure 5.** Percentage change of actual evapotranspiration (AET) and snow depth (SD) from reference (1991-2010) to far-future (2081-2100) periods for the Croche catchment. R and the following number represent the spatial resolution of simulations in $m$.

average amount of snow on the ground decreases by around 40% to 50% according to WaSiM (panels m to p) and Hydrotel (panels i to l) simulations. The considerable reduction of spring freshet between 2081-2100, as seen in Figure 4, is a result of that reduction in snow depth. Since the amount of snow depth reduction in simulations with Hydrotel is higher than in WaSiM (comparing the third and fourth rows in Figure 5), the hydrographs produced by Hydrotlel (Figure 4: panels f and h) are more flattened than those produce by WaSiM (Figure 4: panels b and d).

Changing spatial resolution affects the magnitude of change in the simulation of AET. According to panels a to d and e to f (Figure 5), decreasing spatial resolution corresponds with around a 5 to 15% (depending on the hydrological model) increase of change in the AET. For snow depth, changing spatial resolution has no considerable effect on

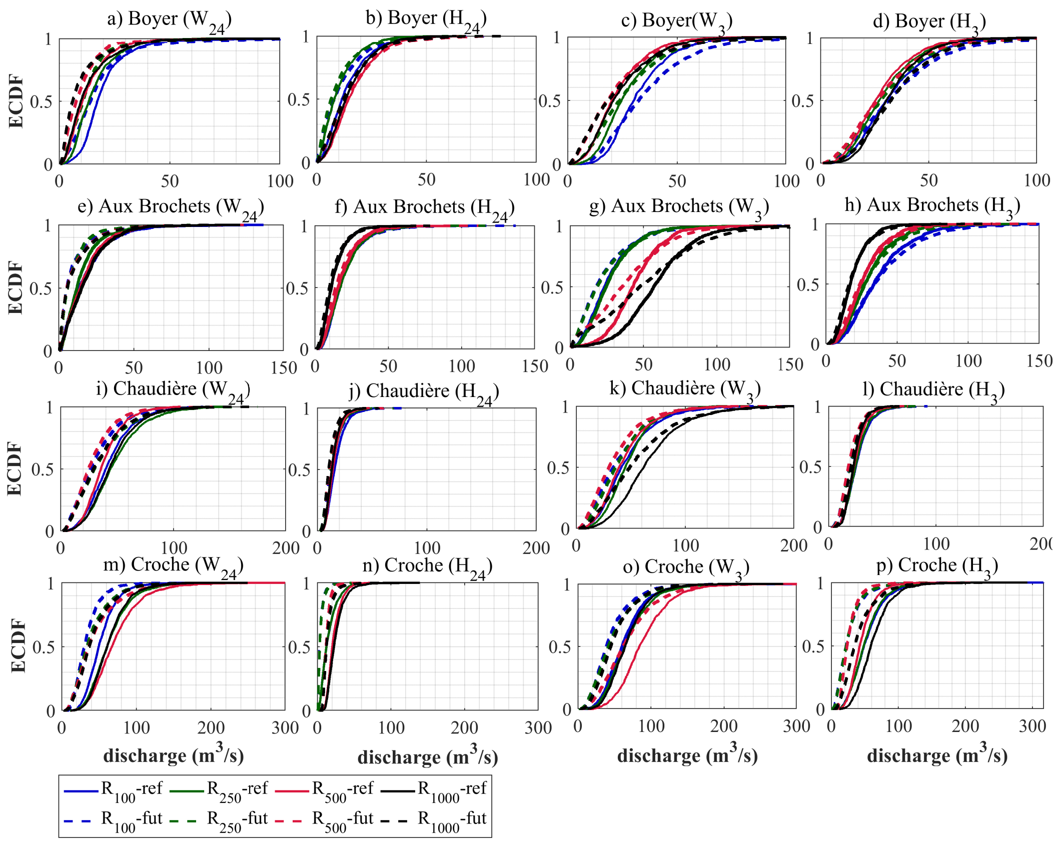


**Figure 6.** Empirical cumulative distribution function (ECDF) of extreme summer-fall flow for reference (ref-solid lines) and future (fut-dashed lines). R and the following number represent the spatial resolution in $m$. W and H are simulations with WaSiM and Hydrotel respectively and their following numbers represent the temporal resolution in an hour

the final results. No significant spatial pattern has been detected for the distribution of AET across the catchment. For snow depth, both models agree on projecting lower values for the southern part with lower altitude illustrating that low-altitude regions are more sensitive to the effect of climate change than high-altitude regions.

### 3.3 Summer-fall extreme flow

Figure 6, shows the empirical cumulative distribution function of maximum summer-fall flow simulated by WaSiM and Hydrotel for the reference and future periods per catchment and resolution. The catchments are ordered in terms of size: the first row shows the results for the smallest catchment and the last row shows the results for the largest. Each spatial resolution is identified by a different color and the future and reference periods are shown in dashed and solid lines respectively. The letters W and H represent WaSiM and Hydrotel respectively, with subscript numbers that indicate the time-step of the simulation (e.g., $W_{24}$ is the WaSiM simulation with a 24-hour time-step.)

A pattern regarding the effect of catchment size and the choice of temporal resolution on the change of extreme flow between the reference and future periods is observable. For small catchments (Boyer and Aux Brochets), by refining the time-step of simulation, there are flow quantiles from which the future extreme flow exceeds that of the reference. This is more clear for WaSiM simulations in panels c) and g). For example, in panel c), when the spatial resolution is 100 $m$, future flows larger than a flood with a 2-year return period (i.e. non-exceedance probability of 0.5) is larger than that of the reference. A similar pattern is also observable for Hydrotel simulations of those catchments (i.e. $d$ and $h$), even though not as clear as WaSiM simulations. By increasing the catchment size (Chaudière and Croche), the graphs show decreasing magnitude of extreme summer-fall flow between the reference and future periods with the same return periods, regardless of temporal resolution. These observations are in accordance with the first hypothesis of this research. Note that the case of Boyer catchments is complicated for very large return periods (¿100-year), as even when the time-step of simulations is 24 hours, the magnitude of a future flood with the same return period exceeds that of the reference period (panels a and b).

For smaller catchments, by changing spatial resolution, the intersection point of future and reference graphs significantly varies. For example, in panel g), with 1000 $m$ spatial resolution, the intersection point is equivalent to a flood with the magnitude of a 3-year return period, but when the spatial resolution is 100 $m$, the intersection point is equivalent to a flood with the magnitude of the 10-year return period. The difference between simulations caused by the change of spatial resolution can also be seen in panels c, k, and o even though the differences between those graphs are smaller. In all cases, whether the time-step of simulation is 3- or 24-hour, simulations by WaSiM have a higher sensitivity to the choice of spatial resolution compared to Hydrotel. These differences illustrate the importance of the choice of spatial resolution and hydrology model. However, no pattern regarding the catchment size and those choices is observable (therefore the second hypothesis cannot be validated from these results).

To further investigate the observations made regarding Figure 6, the relative change of extreme flow for specific quantiles (i.e. flood with 2, 10, 20, and 100-year return periods) is driven and presented in Figure 7. The results are again ordered according to catchment size. As can be observed, the relative change increases when catchment size decreases. Comparing panels b) and d) with panels )a and c) shows that the magnitude of such increase is higher for the 3-hour time-step than for the 24-hour time-step (in accordance with Hypothesis 1). Moreover, for simulations with a 3-hour time-step, the number of pixels with a positive ratio is noticeably higher than with a 24-hour time-step. This demonstrates that the simulated magnitude of flood events with lower return periods in the future increase if a fine temporal resolution is used.

There is no clear pattern regarding the role of spatial resolution in determining the magnitude and direction of change. However, the choice of resolution is not trivial: for example, QT95 in Boyer-R100 (panel a) and QT50 in Boyer-R100 (panel b) undergo a positive change for 100 $m$ resolution but a negative change for all other resolutions. The choice of model has also important implications as the patterns for Hydrotel and WaSiM, particularly for 24-hour simulations, are different. Comparing panels a) and c), Hydrotel produces more simulations with positive relative change than WaSiM. However, WaSiM simulations with positive relative change have a larger magnitude than for Hydrotel. Again these observations confirm the importance of the choice of spatial resolution and hydrology models, but cannot validate the second hypotheses.

### 3.4 Spatial trend

Figures 8 (Boyer) and 9 (Croche) show the spatial distribution of the trend for the maximum annual summer-fall flow simulated by WaSiM, calculated as explained in section 2.5.3, and presented as the percentage of mean annual summer-fall streamflow. This covers the entire simulation period (1991-2100). In this figure, R represents the spatial resolution in $m$, which is followed by the simulation time-step. The hatched area covers the location where the trend is statistically significant at a 5% level ( $p - value <$ 5%).

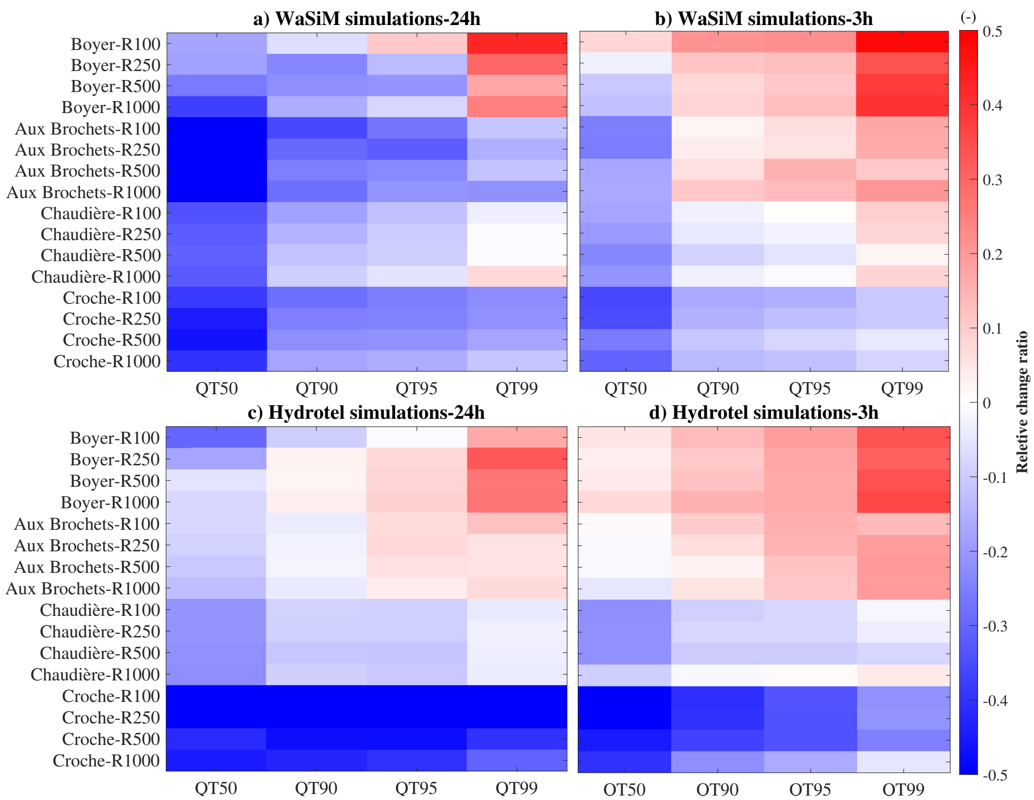


**Figure 7.** Relative change of summer-fall extreme flows (QT50,QT95,. . . ) ordered according to catchment size and spatial resolution.

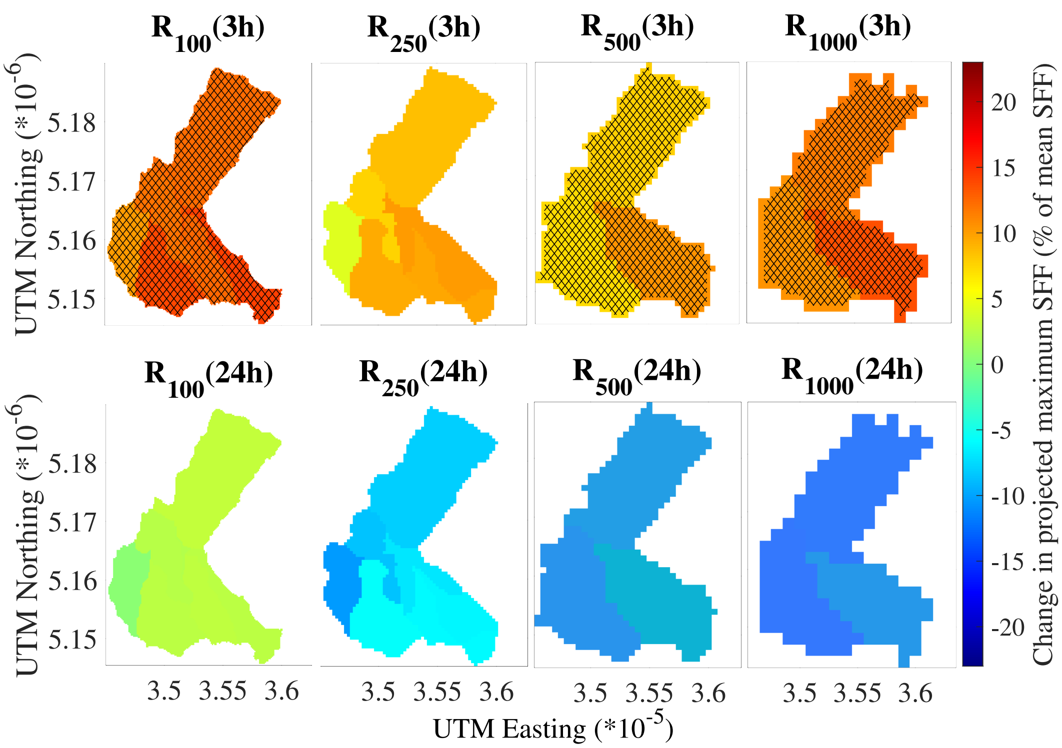


**Figure 8.** The projected change in the annual maximum summer-fall flows (SFF) for the Boyer catchment from 1991 to 2100 (all simulated by WaSiM and expressed by percentage of mean SFF in the reference period). R and the following number represent spatial resolution in $m$. The hatched area covers the area for which the trend is significant at the 5% level according to the Mann-Kendall test.

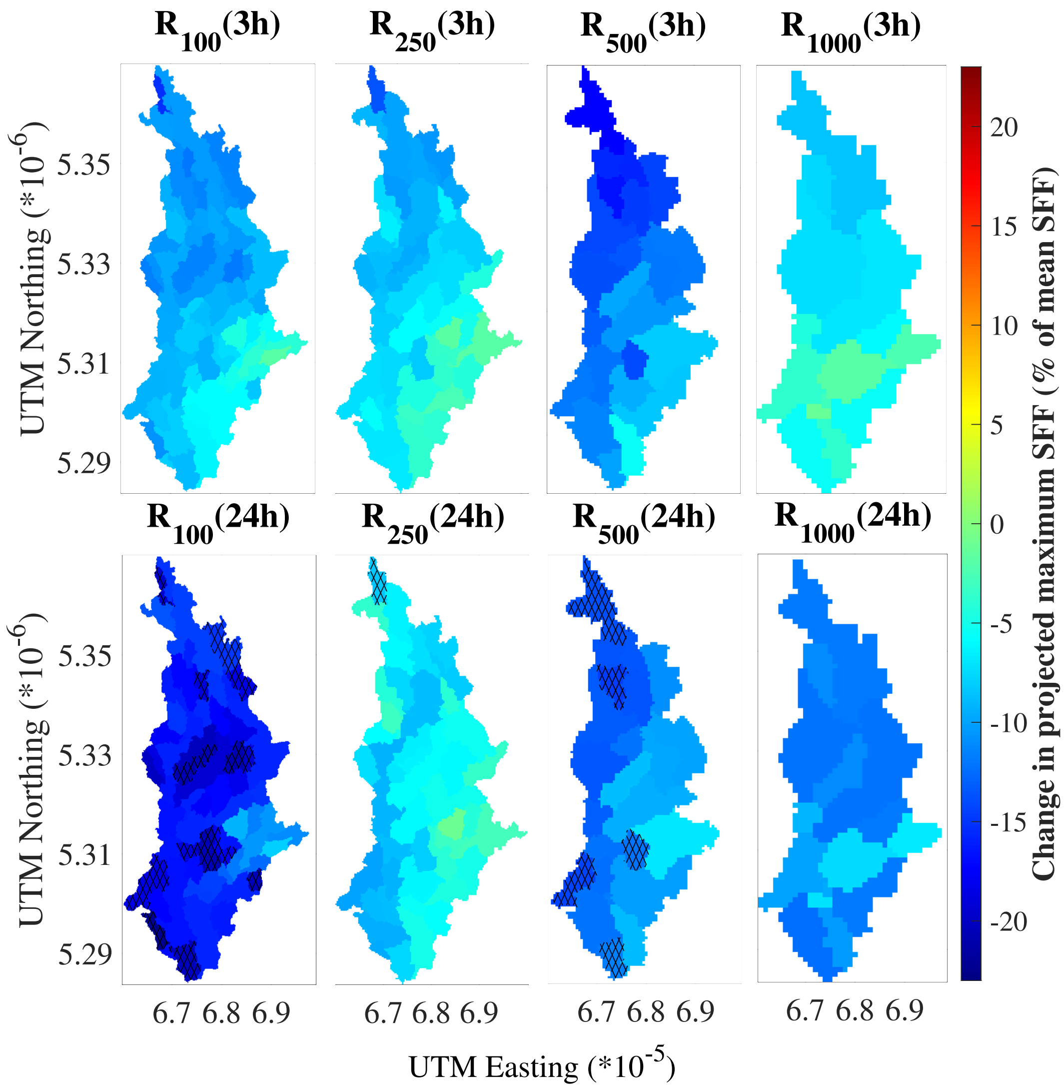


**Figure 9.** The projected change in the annual maximum summer-fall flows (SFF) for the Croche catchment from 1991 to 2100 (all simulated by WaSiM and expressed by percentage of mean SFF in the reference period). R and the following number represent spatial resolution in $m$. The hatched area covers the area for which the trend is significant at the 5% level according to the Mann-Kendall test.

Figure 8 shows that a positive trend holds for all simulations with a 3-hour time-step ($a$ to $d$), regardless of the spatial scale. Moreover, except for $R_{250}(3h)$ (panel a), the trend is significant across most of the catchments. A negative trend emerges across the catchment when the time-step increases (panels e to h), except for the highest (finer) spatial resolution (i.e. $e$: $R_{250}(24h)$) (hypothesis 1). Changing the spatial resolution has important implications here: the average magnitude of the trend across the catchment varies from larger than +5 to more than +20 % for simulations with 3-hour time-step (panels a to d), and from around +3 to less than -10% of that for daily simulations (panels e to h), illustrating large uncertainties in the projection of high flow (hypothesis 2). There is no distinguishable pattern regarding the relationship between the magnitude and direction of the trend and the spatial resolution.

For the Croche catchment, the spatial distribution of the linear trend is negative regardless of the time step and the spatial resolution of the simulations (hypothesis 1). Similar to the Boyer catchment, changing the spatial resolution of the simulations causes large uncertainties: the magnitude of the trend varies from around -5 to -10 % of summer-fall streamflow for a 3-hour time-step (panels a to d), and from less than -5 to around -20 % for daily simulations (panels e to h). Note that like the Boyer catchment, no pattern regarding a relationship between the spatial resolution of simulation and the magnitude of the trend is distinguishable. It appears that by changing the time-step from 3- to 24-hour, larger negative trend values (in terms of magnitude) emerge, showing that the subdaily simulations even influence the trend for the large catchment. The influence, however, is not large enough to change the direction of the trend (hypothesis 1). Note that, unlike the Boyer catchment, the trends calculated for the 3-hour time-step are not significant here.

Observations made in this section are in line with the first hypothesis, as refining the time-step of simulation has mostly influenced the small catchment (i.e., Boyer: Figure 8) rather than the large catchment (i.e., Croche: Figure 9). The second hypothesis cannot be confirmed or rejected with the information provided here.

### 3.5 Variance decomposition

Figure 10 shows the variance decomposition of the relative change in the extreme summer-fall flow into the contribution of spatial resolution, time-step, hydrology model, and their combinations. Results for smaller catchments are shown on the top side and larger catchments are on the bottom side. The spatial resolution has only a minor contribution to the changes for the Boyer catchment. However, this contribution becomes significant when changing the resolution is combined with other factors ( 19% of the variance results from changing the spatial resolution and the hydrology model). For the Aux Brochets catchment, the spatial resolution has a larger contribution to the total variance (15%). This is in line with the results from Figure 6, where the change of spatial resolution created a large difference between simulations. Interestingly, by increasing the catchment size from 584 $km^2$ (Aux Brochets) to 781 $km^2$ (Chaudière) and 1563 $km^2$ (Croche), the contribution of spatial scale in variability, first significantly drops ($< 1\%$) and then increases back to 14%. This clearly suggests a lack of a clear pattern between catchment size and spatial scale (hypothesis 2 regarding spatial scale cannot be verified). The variance obtained from changing the time step is important for all catchments. But similar to spatial scale, a clear relationship between catchment size and time-step cannot be found in this context (hypothesis 2 regarding temporal scale cannot be verified). Changing the hydrology model impacts the variance for the largest catchment (Croche) the most, and loses its contribution by decreasing catchment size (Hypothesis 2 regarding the hydrology model can be verified). Note that the combined effect of simultaneously changing the hydrology model and the temporal or spatial resolution can be an important source of variability, but the combined effect of spatial and temporal scale is not as important.

## 4 Discussion

This study continues our previous research (i.e., Markhali et al., 2022) in quantifying the uncertainty linked to the spatio-temporal representation of catchments in hydrology models. In this research, we did not implement the ensemble method by mixing and matching the parameters and catchment descriptors with different resolutions, due to the computational costs of simulating a large-ensemble of long-duration time series. In the previous study, we learned that the uncertainty linked to the catchment heterogeneity is mostly sensitive to the choice of hydrology model, in the sense that the more sophisticated model in terms of representation of hydrology processes (i.e. WaSiM) cre-

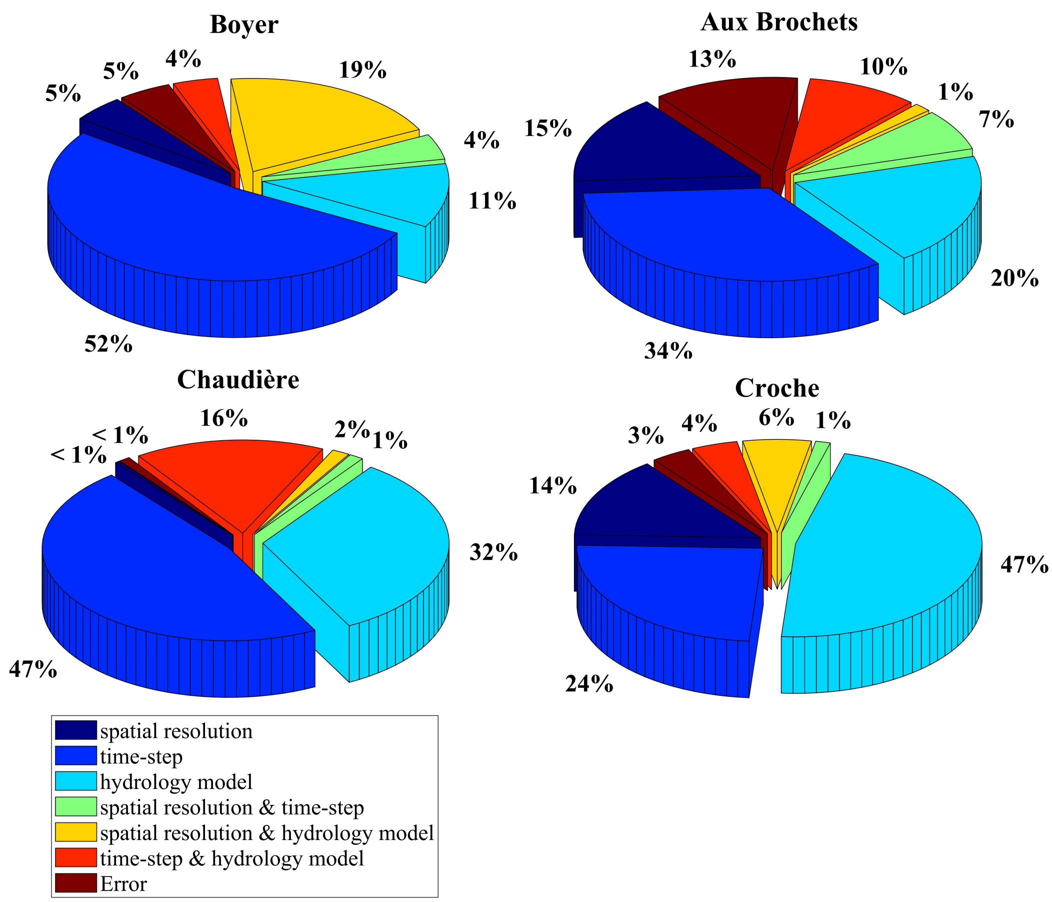


**Figure 10.** Variance decomposition for the relative change in summer-fall extreme flows (average of 2, 10, 20, and 100 yr return periods).

ates larger uncertainties linked to the catchment heterogeneity compared to less sophisticated model (i.e. Hydrotel).

We focused on quantifying that uncertainty in the projection of extreme summer-fall streamflow. We separated catchments based on their surface area. This was necessary because the flood generation mechanism for small and large catchments are different (Blöschl, 2022b). Small catchments are more sensitive to the infiltration excess runoff, while large catchments are sensitive to the saturation excess runoff (Blöschl, 2022a). The results showed that in fact there are relations between the surface area and the choice of time-step and hydrology model in the final response of the catchments: First, using a finer time-step in simulations resulting a statically significant increase in the projection of summer-fall flood hazard in the future for the small but not for the large catchment (Figures 8 and 9). Second, by increasing the catchment area, the contribution of the choice of hydrology model in the uncertainty increased (Figure 10).

The individual contribution of spatial scale is smaller than the other two factors (it is between 1 to 15 % of the total uncertainty according to Figure 10). The question is, whether or not variations of spatial scale should be considered in the simulation for flood projection. To answer this question we investigate the response of the Boyer and Aux Brochets catchments to variation of spatial resolution:

Regarding the Boyer catchment, Figure 10 shows that the joint contribution of spatial resolution and hydrology model in the variation of extreme summer-fall flow reaches up to 19%, which is the highest among all catchments. Also, in Figure 8 e) for WaSim simulations, when the spatial resolution is 100 $m$, the trend is zero or positive across the catchment. However, by lowering the resolution (panels g, h, i), the trend becomes negative. According to Markhali et al. (2022), increasing the spatial resolution causes a non-linear decrease in the coefficient of interflow storage in WaSim for this catchment. This means that the saturation level of the soil is significantly higher for simulation with a 100 $m$ resolution compared to other choices of spatial resolutions. Because of the high value of soil moisture for the simulations with a 100 $m$ resolution and increasing convective rainfall in the future, there is a positive trend in the simulation of high flow even if with a daily simulation time-step. By decreasing the resolution, the interflow storage increases, leading to lower antecedent soil moisture and consequently a negative trend for high flow in the 24-hour time step.

The Aux Brochets catchment shows the largest sensitivity to the spatio-temporal resolution in flood projection (Figure 6). Coarsening the spatial resolution in WaSiM induces modifications to the slopes of this catchment in the model, which in turn causes a reorientation of surface and subsurface flows. This results in soil saturation in a portion of the catchment leading to the outlet (Markhali et al., 2022). High antecedent soil moisture combined with convective storms results in a rapid response of the catchment for simulations with low spatial but high temporal resolutions. The significantly larger magnitude of flood for the simulations with a 3-hour time-step and a spatial resolution of 500 to 1000 $m$ (the red and black lines in Figure 6 *b*) could be attributed to the mechanism explained above. The decomposition of the variance for this catchment in Figure 10 confirms that the contribution of the spatial scale individually or together with the other factors explains 23% of the total variance, which is higher than two other larger catchments.

Among all the catchments studied here, the Boyer catchment has the maximum human intervention in terms of deforestation and agriculture (Markhali et al., 2022). Also, Aux Brochets is a flat catchment with uneven areas (hills and valleys). This type of topography is more difficult to represent in hydrology models. Therefore, the hydrology model's structure and the degree to which that model reflects the details of topographic and land-use characteristics are important factors to consider. This study suggests accounting for the variation of spatial resolution for flat catchments or catchments with high agricultural lands if a distributed hydrology model with a high level of sophistication in representing hydrological processes should be used.

The intensive computational demand of the two distributed process-based hydrology models used in this research limits the number of catchments that could be included. There is an opportunity to work towards generalizing the conclusions of this research by involving a higher number of catchments, with different sizes and land uses. Moreover, adding more hydrology models with various structures seems necessary to gain more in-depth knowledge about the effect of the choice of process-based hydrology models in flood projection. Furthermore, the recent advances in increasing the spatial and temporal resolution of RCMs are appealing to further investigate the impact of spatio-temporal resolution in climate impact studies. Recent models with a high spatial resolution (¡4km) have shown promise in the simulation of convective-driven rainfall (Lucas-Picher et al., 2021). The problem with using these models is the large capacity required for their data (Gutowski et al., 2020). Also, coupling them with distributed hydrology models adds to the computational costs of the modeling. Further advancement in computational power and data storage is required for the application of these models in impact studies (Schär et al., 2020).

## 5 Conclusion

This study investigated the role of spatio-temporal resolution of simulations, the choice of hydrology model, and the catchment size in determining the change of extreme summer-fall flow in the future under climate change. A large-ensemble regional climate model simulation (ClimEx) was bias corrected by multi-variate bias correction (MBCn) and coupled with two distributed hydrology models (WaSiM and Hydrotel) to simulate streamflow over four catchments with different sizes across Quebec. Simulations have been conducted for different spatial (100, 250, 500, 1000 $m$) and temporal (24- and 3-hour time-steps) resolutions. Multiple experiments have been conducted to reject/validate two main hypotheses: 1) For small catchments, by increasing temporal resolution, the simulated extreme summer-fall flow in the future period becomes larger than that of the reference period. 2) The change in the spatio-temporal scale of modeling causes variability in the projection of extreme flow. By increasing the catchment size, the contribution of the choice of hydrology model and spatial scale in that variability increases, and that of the time-scale decreases.

The experiments show that:

- A pattern regarding catchment size and temporal resolution exists: simulations with 3-hour time-steps (Figures 6, 7, 8) predict that extreme summer-fall flow will increase in the far-future for small catchments, regardless of model and spatial resolution. Therefore, the first hypothesis is verified for this case study. Moreover, the choice of a simulation time step is a major determinant in the variability of flood projection for small catchments and by increasing catchment size, its influence decreases (Figure 10). As a result, part of the second hypothesis concerning the relationship between temporal resolution and small catchments is also verified for this case study.
- For large catchments, the choice of spatial resolution has a larger contribution in the simulation of extreme summer-fall flood (Figures 6 and 10). This however does not exceed the contribution of the choice of time-step (Figure 10). Moreover, if the time-step is 24-hour, it is likely that the spatial resolution changes the direction of the trend for small catchments (Figures 8 and 9 and section 4). Therefore, part of the second hypothesis concerning the impact of spatial resolution on large catchments cannot be verified here.
- The choice of a hydrology model can be important for both small and large catchments. It appears that by increasing the catchment's size this choice becomes more

important (e.g., Figure 8 and 10). Therefore, part of the second hypothesis regarding the impact of the choice of a hydrology model on large catchments can be verified here. In all cases, WaSiM shows a higher variance than Hydrotel for streamflow projections (Figure 6).

## References


Aalbers, E. E., Lenderink, G., van Meijgaard, E., & van den Hurk, B. J. (2018). Local-scale changes in mean and heavy precipitation in western europe, climate change or internal variability? *Climate Dynamics*, *50*(11), 4745–4766.

Addor, N., Rössler, O., Köplin, N., Huss, M., Weingartner, R., & Seibert, J. (2014). Robust changes and sources of uncertainty in the projected hydrological regimes of swiss catchments. *Water Resources Research*, *50*(10), 7541–7562. Retrieved from https://doi.org/10.1002/2014WR015549

Alexander, L. V., Zhang, X., Peterson, T. C., Caesar, J., Gleason, B., Klein Tank, A., ... others (2006). Global observed changes in daily climate extremes of temperature and precipitation. *Journal of Geophysical Research: Atmospheres*, *111*(D5).

Ali, R., Kuriqi, A., Abubaker, S., & Kisi, O. (2019). Long-term trends and seasonality detection of the observed flow in yangtze river using mann-kendall and sen's innovative trend method. *Water*, *11*(9), 1855.

Barnes, E. A., & Barnes, R. J. (2015). Estimating linear trends: simple linear regression versus epoch differences. *Journal of Climate*, *28*(24), 9969–9976.

Beven, K. (1997). Topmodel: a critique. *Hydrological processes*, *11*(9), 1069–1085.

Beven, K. (2019). How to make advances in hydrological modelling. *Hydrology Research*, *50*(6), 1481–1494.

Beven, K. J. (2000). Uniqueness of place and process representations in hydrological modelling. *Hydrology and earth system sciences*, *4*(2), 203–213. Retrieved from https://doi.org/10.5194/hess-4-203-2000

Blöschl, G. (2022a). Flood generation: process patterns from the raindrop to the ocean. *Hydrology and Earth System Sciences*, *26*(9), 2469–2480.

Blöschl, G. (2022b). Three hypotheses on changing river flood hazards. *Hydrology and Earth System Sciences Discussions*, 1–37.

Blöschl, G., Bierkens, M. F., Chambel, A., Cudennec, C., Destouni, G., Fiori, A., ... others (2019). Twenty-three unsolved problems in hydrology (uph)–a community perspective. *Hydrological Sciences Journal*, *64*(10), 1141–1158. Retrieved from https://doi.org/10.1080/02626667.2019.1620507

Blöschl, G., Bloschl, G., Sivapalan, M., Wagener, T., Savenije, H., & Viglione, A. (2013). *Runoff prediction in ungauged basins: synthesis across processes, places and scales*. Cambridge University Press.

Blöschl, G., & Sivapalan, M. (1995). Scale issues in hydrological modelling: a review. *Hydrological processes*, *9*(3-4), 251–290.

Bormann, H., Breuer, L., Gräff, T., Huisman, J., & Croke, B. (2009). Assessing the impact of land use change on hydrology by ensemble modelling (luchem) iv: Model sensitivity to data aggregation and spatial (re-) distribution. *Advances in water resources*, *32*(2), 171–192. Retrieved from https://doi.org/10.1016/j.advwatres.2008.01.002

Breinl, K., Lun, D., Müller-Thomy, H., & Blöschl, G. (2021). Understanding the relationship between rainfall and flood probabilities through combined intensity-duration-frequency analysis. *Journal of Hydrology*, *602*, 126759.

Breuer, L., Huisman, J., Willems, P., Bormann, H., Bronstert, A., Croke, B., ... others (2009). Assessing the impact of land use change on hydrology by ensemble modeling (luchem). i: Model intercomparison with current land use. *Advances in Water Resources*, *32*(2), 129–146. Retrieved from https://doi.org/10.1016/j.advwatres.2008.10.003

Brown, A. E., Zhang, L., McMahon, T. A., Western, A. W., & Vertessy, R. A. (2005). A review of paired catchment studies for determining changes in water yield resulting from alterations in vegetation. *Journal of hydrology*, *310*(1-4), 28–61.

Cannon, A. J. (2018). Multivariate quantile mapping bias correction: an n-dimensional probability density function transform for climate model simulations of multiple variables. *Climate dynamics*, *50*(1), 31–49.

Cannon, A. J., Piani, C., & Sippel, S. (2020). Bias correction of climate model output for impact models. In *Climate extremes and their implications for impact and risk assessment* (pp. 77–104). Elsevier.

Cao, X., Lyu, H., Ni, G., Tian, F., Ma, Y., & Grimmond, C. (2020). Spatial scale effect of surface routing and its parameter upscaling for urban flood simulation using a grid-based model. *Water Resources Research*, *56*(2), e2019WR025468. Retrieved from https://doi.org/10.1029/2019WR025468

Clark, M. P., Bierkens, M. F., Samaniego, L., Woods, R. A., Uijlenhoet, R., Bennett, K. E., ... Peters-Lidard, C. D. (2017). The evolution of process-based hydrologic models: historical challenges and the collective quest for physical realism. *Hydrology and Earth System Sciences (Online)*, *21*(LA-UR-17-27603). Retrieved from https://doi.org/10.5194/hess-21-3427-2017

Clark, M. P., Nijssen, B., Lundquist, J. D., Kavetski, D., Rupp, D. E., Woods, R. A., ... others (2015). A unified approach for process-based hydrologic modeling: 1. modeling concept. *Water Resources Research*, *51*(4), 2498–2514. Retrieved from https://doi.org/10.1002/2015WR017200

Contractor, S., Donat, M. G., & Alexander, L. V. (2021). Changes in observed daily precipitation over global land areas since 1950. *Journal of Climate*, *34*(1), 3–19.

Dembélé, M., Hrachowitz, M., Savenije, H. H., Mariéthoz, G., & Schaefli, B. (2020). Improving the predictive skill of a distributed hydrological model by calibration on spatial patterns with multiple satellite data sets. *Water resources research*, *56*(1), e2019WR026085. Retrieved from https://doi.org/10.1029/2019WR026085

Deser, C., Knutti, R., Solomon, S., & Phillips, A. S. (2012). Communication of the role of natural variability in future north american climate. *Nature Climate Change*, *2*(11), 775.

Deser, C., Phillips, A., Bourdette, V., & Teng, H. (2012). Uncertainty in climate change projections: the role of internal variability. *Climate dynamics*, *38*(3-4), 527–546.

Ding, Q., & Steig, E. J. (2013). Temperature change on the antarctic peninsula linked to the tropical pacific. *Journal of Climate*, *26*(19), 7570–7585.

Do, H. X., Zhao, F., Westra, S., Leonard, M., Gudmundsson, L., Boulange, J. E. S., ... others (2020). Historical and future changes in global flood magnitude–evidence from a model–observation investigation. *Hydrology and Earth System Sciences*, *24*(3), 1543–1564.

Donat, M., Alexander, L. V., Yang, H., Durre, I., Vose, R., Dunn, R. J., ... others (2013). Updated analyses of temperature and precipitation extreme indices since the beginning of the twentieth century: The hadex2 dataset. *Journal of Geophysical Research: Atmospheres*, *118*(5), 2098–2118.

Donat, M. G., Lowry, A. L., Alexander, L. V., O'Gorman, P. A., & Maher, N. (2016). More extreme precipitation in the world's dry and wet regions. *Nature Climate Change*, *6*(5), 508.

Dooge, J. C. (1986). Looking for hydrologic laws. *Water Resources Research*, *22*(9S), 46S–58S. Retrieved from https://doi.org/10.1029/WR022i09Sp0046S

Duethmann, D., Blöschl, G., & Parajka, J. (2020). Why does a conceptual hydrological model fail to correctly predict discharge changes in response to climate change? *Hydrology and Earth System Sciences*, *24*(7), 3493–3511.

Dunne, T., & Black, R. D. (1970). Partial area contributions to storm runoff in a small new england watershed. *Water resources research*, *6*(5), 1296–1311.

Faghih, M., Brissette, F., & Sabeti, P. (2022). Impact of correcting sub-daily climate model biases for hydrological studies. *Hydrology and Earth System Sciences*, *26*(6), 1545–1563.

Field, C. B., Barros, V., Stocker, T. F., & Dahe, Q. (2012). *Managing the risks of extreme events and disasters to advance climate change adaptation: special report of the intergovernmental panel on climate change.* Cambridge University Press.

Fortin, J.-P., Turcotte, R., Massicotte, S., Moussa, R., Fitzback, J., & Villeneuve, J.-P. (2001a). Distributed watershed model compatible with remote sensing and gis data. ii: Application to chaudière watershed. *Journal of Hydrologic Engineering*, *6*(2), 100–108. Retrieved from `https://doi.org/10.1061/(ASCE)1084-0699(2001)6:2(91)`

Fortin, J.-P., Turcotte, R., Massicotte, S., Moussa, R., Fitzback, J., & Villeneuve, J.-P. (2001b). Distributed watershed model compatible with remote sensing and gis data. ii: Application to chaudière watershed. *Journal of Hydrologic Engineering*, *6*(2), 100–108. Retrieved from `https://doi.org/10.1061/(ASCE)1084-0699(2001)6:2(100)`

Fowler, H. J., Ali, H., Allan, R. P., Ban, N., Barbero, R., Berg, P., . . . others (2021). Towards advancing scientific knowledge of climate change impacts on short-duration rainfall extremes. *Philosophical Transactions of the Royal Society A*, *379*(2195), 20190542.

François, B., Schlef, K., Wi, S., & Brown, C. (2019). Design considerations for riverine floods in a changing climate–a review. *Journal of Hydrology*, *574*, 557–573.

Freeze, R. A., & Harlan, R. (1969). Blueprint for a physically-based, digitally-simulated hydrologic response model. *Journal of hydrology*, *9*(3), 237–258.

Gebremicael, T., Mohamed, Y., & Van der Zaag, P. (2019). Attributing the hydrological impact of different land use types and their long-term dynamics through combining parsimonious hydrological modelling, alteration analysis and plsr analysis. *Science of the Total Environment*, *660*, 1155–1167.

Golden, H. E., & Knightes, C. D. (2011). Simulated watershed mercury and nitrate flux responses to multiple land cover conversion scenarios. *Environmental Toxicology and Chemistry*, *30*(4), 773–786.

Gomi, T., Sidle, R. C., & Richardson, J. S. (2002). Understanding processes and downstream linkages of headwater systems: headwaters differ from downstream reaches by their close coupling to hillslope processes, more temporal and spatial variation, and their need for different means of protection from land use. *BioScience*, *52*(10), 905–916.

Gupta, H. V., Kling, H., Yilmaz, K. K., & Martinez, G. F. (2009). Decomposition of the mean squared error and nse performance criteria: Implications for improving hydrological modelling. *Journal of hydrology*, *377*(1-2), 80–91. Retrieved from `https://doi.org/10.1016/j.jhydrol.2009.08.003`

Gutowski, W. J., Ullrich, P. A., Hall, A., Leung, L. R., O'Brien, T. A., Patricola, C. M., . . . others (2020). The ongoing need for high-resolution regional climate models: Process understanding and stakeholder information. *Bulletin of the American Meteorological Society*, *101*(5), E664–E683.

Hamon, W. R. (1961). Estimating potential evapotranspiration. *Journal of the Hydraulics Division*, *87*(3), 107–120. Retrieved from `https://doi.org/10.1061/JYCEAJ.0000599`

Hersbach, H., Bell, B., Berrisford, P., Hirahara, S., Horányi, A., Muñoz-Sabater, J., . . . others (2020). The era5 global reanalysis. *Quarterly Journal of the Royal Meteorological Society*, *146*(730), 1999–2049.

Horton, R. E. (1933). The role of infiltration in the hydrologic cycle. *Eos, Transactions American Geophysical Union*, *14*(1), 446–460.

Huisman, J., Breuer, L., Bormann, H., Bronstert, A., Croke, B., Frede, H.-G., … others (2009). Assessing the impact of land use change on hydrology by ensemble modeling (luchem) iii: Scenario analysis. *Advances in Water Resources*, *32*(2), 159–170. Retrieved from https://doi.org/10.1016/j.advwatres.2008.06.009

Huot, P.-L., Poulin, A., Audet, C., & Alarie, S. (2019). A hybrid optimization approach for efficient calibration of computationally intensive hydrological models. *Hydrological Sciences Journal*(just-accepted).

Ichiba, A., Gires, A., Tchiguirinskaia, I., Schertzer, D., Bompard, P., & Veldhuis, M.-C. T. (2018). Scale effect challenges in urban hydrology highlighted with a distributed hydrological model. *Hydrology and Earth System Sciences*, *22*(1), 331–350. Retrieved from https://doi.org/10.5194/hess-22-331-2018

Jencso, K. G., McGlynn, B. L., Gooseff, M. N., Bencala, K. E., & Wondzell, S. M. (2010). Hillslope hydrologic connectivity controls riparian groundwater turnover: Implications of catchment structure for riparian buffering and stream water sources. *Water Resources Research*, *46*(10).

Kendon, E. J., Ban, N., Roberts, N. M., Fowler, H. J., Roberts, M. J., Chan, S. C., … Wilkinson, J. M. (2017). Do convection-permitting regional climate models improve projections of future precipitation change? *Bulletin of the American Meteorological Society*, *98*(1), 79–93.

Koci, J., Sidle, R. C., Jarihani, B., & Cashman, M. J. (2020). Linking hydrological connectivity to gully erosion in savanna rangelands tributary to the great barrier reef using structure-from-motion photogrammetry. *Land Degradation & Development*, *31*(1), 20–36.

Krebs, G., Kokkonen, T., Valtanen, M., Setälä, H., & Koivusalo, H. (2014). Spatial resolution considerations for urban hydrological modelling. *Journal of Hydrology*, *512*, 482–497. Retrieved from https://doi.org/10.1016/j.jhydrol.2014.03.013

Leduc, M., Mailhot, A., Frigon, A., Martel, J.-L., Ludwig, R., Brietzke, G. B., … others (2019). The climex project: a 50-member ensemble of climate change projections at 12-km resolution over europe and northeastern north america with the canadian regional climate model (crcm5). *Journal of Applied Meteorology and Climatology*, *58*(4), 663–693.

Li, Y., Chang, J., Luo, L., Wang, Y., Guo, A., Ma, F., & Fan, J. (2019). Spatiotemporal impacts of land use land cover changes on hydrology from the mechanism perspective using swat model with time-varying parameters. *Hydrology Research*, *50*(1), 244–261. Retrieved from https://doi.org/10.2166/nh.2018.006

Lochbihler, K., Lenderink, G., & Siebesma, A. P. (2017). The spatial extent of rainfall events and its relation to precipitation scaling. *Geophysical Research Letters*, *44*(16), 8629–8636.

López-Vicente, M., Sun, X., Onda, Y., Kato, H., Gomi, T., & Hiraoka, M. (2017). Effect of tree thinning and skidding trails on hydrological connectivity in two japanese forest catchments. *Geomorphology*, *292*, 104–114.

Lucas-Picher, P., Argüeso, D., Brisson, E., Tramblay, Y., Berg, P., Lemonsu, A., … Caillaud, C. (2021). Convection-permitting modeling with regional climate models: Latest developments and next steps. *Wiley Interdisciplinary Reviews: Climate Change*, *12*(6), e731.

Lucas-Picher, P., Lachance-Cloutier, S., Arsenault, R., Poulin, A., Ricard, S., Turcotte, R., & Brissette, F. (2020). Will evolving climate conditions increase the risk of floods of the large us-canada transboundary richelieu river basin? *JAWRA Journal of the American Water Resources Association*. Retrieved from https://doi.org/10.1111/1752-1688.12891

Markhali, S. P., Poulin, A., & Boucher, M.-A. (2022). Spatio-temporal discretization uncertainty of distributed hydrological models. *Hydrological Processes*, e14635.

Martel, J.-L., Brissette, F., & Poulin, A. (2020). Impact of the spatial density of weather stations on the performance of distributed and lumped hydrological models. *Canadian Water Resources Journal/Revue canadienne des ressources hydriques*, 1–14. Retrieved from `https://doi.org/10.5194/gmd-12-2501-2019`

Martel, J.-L., Brissette, F. P., Lucas-Picher, P., Troin, M., & Arsenault, R. (2021). Climate change and rainfall intensity-duration-frequency curves: Overview of science and guidelines for adaptation. *Journal of Hydrologic Engineering*, *26*(10).

Martel, J.-L., Mailhot, A., & Brissette, F. (2020). Global and regional projected changes in 100-yr subdaily, daily, and multiday precipitation extremes estimated from three large ensembles of climate simulations. *Journal of Climate*, *33*(3), 1089–1103.

Masson-Delmotte, V., Zhai, P., Pirani, A., Connors, S. L., Péan, C., Berger, S., ... others (2021). Climate change 2021: the physical science basis. *Contribution of working group I to the sixth assessment report of the intergovernmental panel on climate change*, 2.

Mearns, L., McGinnis, S., Korytina, D., Arritt, R., Biner, S., Bukovsky, M., ... others (2017). *The na-cordex dataset, version 1.0. ncar climate data gateway, boulder co.*

Meresa, H., Tischbein, B., Mendela, J., Demoz, R., Abreha, T., Weldemichael, M., & Ogbu, K. (2022). The role of input and hydrological parameters uncertainties in extreme hydrological simulations. *Natural Resource Modeling*, *35*(1), e12320.

Meresa, H. K., & Romanowicz, R. J. (2017). The critical role of uncertainty in projections of hydrological extremes. *Hydrology and Earth System Sciences*, *21*(8), 4245–4258.

Merz, B., Blöschl, G., Vorogushyn, S., Dottori, F., Aerts, J. C., Bates, P., ... others (2021). Causes, impacts and patterns of disastrous river floods. *Nature Reviews Earth & Environment*, *2*(9), 592–609.

Meyer, J., Kohn, I., Stahl, K., Hakala, K., Seibert, J., & Cannon, A. J. (2019). Effects of univariate and multivariate bias correction on hydrological impact projections in alpine catchments. *Hydrology and Earth System Sciences*, *23*(3), 1339–1354.

Min, S.-K., Zhang, X., Zwiers, F. W., & Hegerl, G. C. (2011). Human contribution to more-intense precipitation extremes. *Nature*, *470*(7334), 378.

Molnar, P., Fatichi, S., Gaál, L., Szolgay, J., & Burlando, P. (2015). Storm type effects on super clausius–clapeyron scaling of intense rainstorm properties with air temperature. *Hydrology and Earth System Sciences*, *19*(4), 1753–1766.

Montanari, A., & Koutsoyiannis, D. (2014). Modeling and mitigating natural hazards: Stationarity is immortal! *Water resources research*, *50*(12), 9748–9756.

Montgomery, D. C. (2017). *Design and analysis of experiments*. John wiley & sons.

Mooney, P., Broderick, C., Bruyère, C., Mulligan, F., & Prein, A. (2017). Clustering of observed diurnal cycles of precipitation over the united states for evaluation of a wrf multiphysics regional climate ensemble. *Journal of Climate*, *30*(22), 9267–9286.

Noguchi, S., Tsuboyama, Y., Sidle, R. C., & Hosoda, I. (1999). Morphological characteristics of macropores and the distribution of preferential flow pathways in a forested slope segment. *Soil Science Society of America Journal*, *63*(5), 1413–1423.

Pandey, B. K., Khare, D., Kawasaki, A., & Mishra, P. K. (2019). Climate change impact assessment on blue and green water by coupling of representative cmip5 climate models with physical based hydrological model. *Water resources*

*management*, *33*(1), 141–158.
Prein, A. F., Langhans, W., Fosser, G., Ferrone, A., Ban, N., Goergen, K., … others (2015). A review on regional convection-permitting climate modeling: Demonstrations, prospects, and challenges. *Reviews of geophysics*, *53*(2), 323–361.
Refsgaard, C. (1995). Mike she. *Computer models of catchment hydrology*, 809–846. Retrieved from https://scholar.google.ca/scholar?hl=en&as_sdt=0%2C5&as_vis=1&q=Mike+she&btnG=
Sanderson, B. M., Oleson, K. W., Strand, W. G., Lehner, F., & O'Neill, B. C. (2018). A new ensemble of gcm simulations to assess avoided impacts in a climate mitigation scenario. *Climatic Change*, *146*(3-4), 303–318.
Savenije, H. H., & Hrachowitz, M. (2017). Hess opinions catchments as meta-organisms–a new blueprint for hydrological modelling. *Hydrology and Earth System Sciences*, *21*(2), 1107–1116.
Schär, C., Fuhrer, O., Arteaga, A., Ban, N., Charpilloz, C., Di Girolamo, S., … others (2020). Kilometer-scale climate models: Prospects and challenges. *Bulletin of the American Meteorological Society*, *101*(5), E567–E587.
Schulla, J., & Jasper, K. (2007). Model description wasim-eth. *Institute for Atmospheric and Climate Science, Swiss Federal Institute of Technology, Zürich*. Retrieved from https://scholar.google.ca/scholar?hl=en&as_sdt=0%2C5&as_vis=1&q=Model+description+wasim-eth&btnG=
Sidle, R. C. (2006). Field observations and process understanding in hydrology: essential components in scaling. *Hydrological Processes*, *20*(6), 1439–1445.
Sidle, R. C. (2021). Strategies for smarter catchment hydrology models: incorporating scaling and better process representation. *Geoscience Letters*, *8*(1), 1–14.
Sidle, R. C., Gomi, T., Usuga, J. C. L., & Jarihani, B. (2017). Hydrogeomorphic processes and scaling issues in the continuum from soil pedons to catchments. *Earth-Science Reviews*, *175*, 75–96.
Singh, H. V., Kalin, L., Morrison, A., Srivastava, P., Lockaby, G., & Pan, S. (2015). Post-validation of swat model in a coastal watershed for predicting land use/cover change impacts. *Hydrology Research*, *46*(6), 837–853. Retrieved from https://doi.org/10.2166/nh.2015.222
Sivapalan, M., & Blöschl, G. (2015). Time scale interactions and the coevolution of humans and water. *Water Resources Research*, *51*(9), 6988–7022.
Swain, D., Wing, O. E., Bates, P. D., Done, J., Johnson, K., & Cameron, D. (2020). Increased flood exposure due to climate change and population growth in the united states. *Earth's Future*, *8*(11), e2020EF001778.
Swart, N. C., Cole, J. N., Kharin, V. V., Lazare, M., Scinocca, J. F., Gillett, N. P., … others (2019). The canadian earth system model version 5 (canesm5. 0.3). *Geoscientific Model Development*, *12*(11), 4823–4873.
Tarek, M., Brissette, F. P., & Arsenault, R. (2020). Evaluation of the era5 reanalysis as a potential reference dataset for hydrological modelling over north america. *Hydrology and Earth System Sciences*, *24*(5), 2527–2544. Retrieved from https://doi.org/10.5194/hess-24-2527-2020
Tavangar, S., Moradi, H., Massah Bavani, A., & Gholamalifard, M. (2019). A futuristic survey of the effects of lu/lc change on stream flow by ca–markov model: a case of the nekarood watershed, iran. *Geocarto International*, 1–17. Retrieved from https://doi.org/10.1080/10106049.2019.1633419
Tolson, B. A., & Shoemaker, C. A. (2007). Dynamically dimensioned search algorithm for computationally efficient watershed model calibration. *Water Resources Research*, *43*(1). Retrieved from https://doi.org/10.1029/2005WR004723
Turcotte, B., Morse, B., & Pelchat, G. (2020). Impact of climate change on the frequency of dynamic breakup events and on the risk of ice-jam floods in quebec, canada. *Water*, *12*(10), 2891. Retrieved from https://doi.org/10.3390/

w12102891
Viglione, A., & Blöschl, G. (2009). On the role of storm duration in the mapping of rainfall to flood return periods. *Hydrology and Earth System Sciences*, *13*(2), 205–216.
Viglione, A., Chirico, G. B., Woods, R., & Blöschl, G. (2010). Generalised synthesis of space–time variability in flood response: An analytical framework. *Journal of Hydrology*, *394*(1-2), 198–212.
Viglione, A., Merz, B., Viet Dung, N., Parajka, J., Nester, T., & Blöschl, G. (2016). Attribution of regional flood changes based on scaling fingerprints. *Water resources research*, *52*(7), 5322–5340.
Viney, N. R., Bormann, H., Breuer, L., Bronstert, A., Croke, B. F., Frede, H., … others (2009). Assessing the impact of land use change on hydrology by ensemble modelling (luchem) ii: Ensemble combinations and predictions. *Advances in water resources*, *32*(2), 147–158. Retrieved from https://doi.org/10.1016/j.advwatres.2008.05.006
Wang, F., Huang, G., Fan, Y., & Li, Y. (2020). Robust subsampling anova methods for sensitivity analysis of water resource and environmental models. *Water Resources Management*, *34*(10), 3199–3217.
Warsta, L., Niemi, T. J., Taka, M., Krebs, G., Haahti, K., Koivusalo, H., & Kokkonen, T. (2017). Development and application of an automated subcatchment generator for swmm using open data. *Urban Water Journal*, *14*(9), 954–963. Retrieved from https://doi.org/10.1080/1573062X.2017.1325496
Westra, S., Alexander, L. V., & Zwiers, F. W. (2013). Global increasing trends in annual maximum daily precipitation. *Journal of climate*, *26*(11), 3904–3918.
Westra, S., Fowler, H., Evans, J., Alexander, L., Berg, P., Johnson, F., … Roberts, N. (2014). Future changes to the intensity and frequency of short-duration extreme rainfall. *Reviews of Geophysics*, *52*(3), 522–555.
Woods, R., & Sivapalan, M. (1999). A synthesis of space-time variability in storm response: Rainfall, runoff generation, and routing. *Water Resources Research*, *35*(8), 2469–2485.
Yang, W., Long, D., & Bai, P. (2019). Impacts of future land cover and climate changes on runoff in the mostly afforested river basin in north china. *Journal of Hydrology*, *570*, 201–219. Retrieved from https://doi.org/10.1016/j.jhydrol.2018.12.055
Yin, J., Gentine, P., Zhou, S., Sullivan, S. C., Wang, R., Zhang, Y., & Guo, S. (2018). Large increase in global storm runoff extremes driven by climate and anthropogenic changes. *Nature communications*, *9*(1), 1–10. Retrieved from https://doi.org/10.1038/s41467-018-06765-2
Zhang, L., Nan, Z., Yu, W., Zhao, Y., & Xu, Y. (2018). Comparison of baseline period choices for separating climate and land use/land cover change impacts on watershed hydrology using distributed hydrological models. *Science of the Total Environment*, *622*, 1016–1028.
Zhong, R., He, Y., & Chen, X. (2018). Responses of the hydrological regime to variations in meteorological factors under climate change of the tibetan plateau. *Atmospheric Research*, *214*, 296–310.
Zhou, Z., Smith, J. A., Yang, L., Baeck, M. L., Chaney, M., Ten Veldhuis, M.-C., … Liu, S. (2017). The complexities of urban flood response: Flood frequency analyses for the charlotte metropolitan region. *Water Resources Research*, *53*(8), 7401–7425. Retrieved from https://doi.org/10.1002/2016WR019997
Zhuan, M.-J., Chen, J., Shen, M.-X., Xu, C.-Y., Chen, H., & Xiong, L.-H. (2018). Timing of human-induced climate change emergence from internal climate variability for hydrological impact studies. *Hydrology Research*, *49*(2), 421–437.

**Figure 1.**

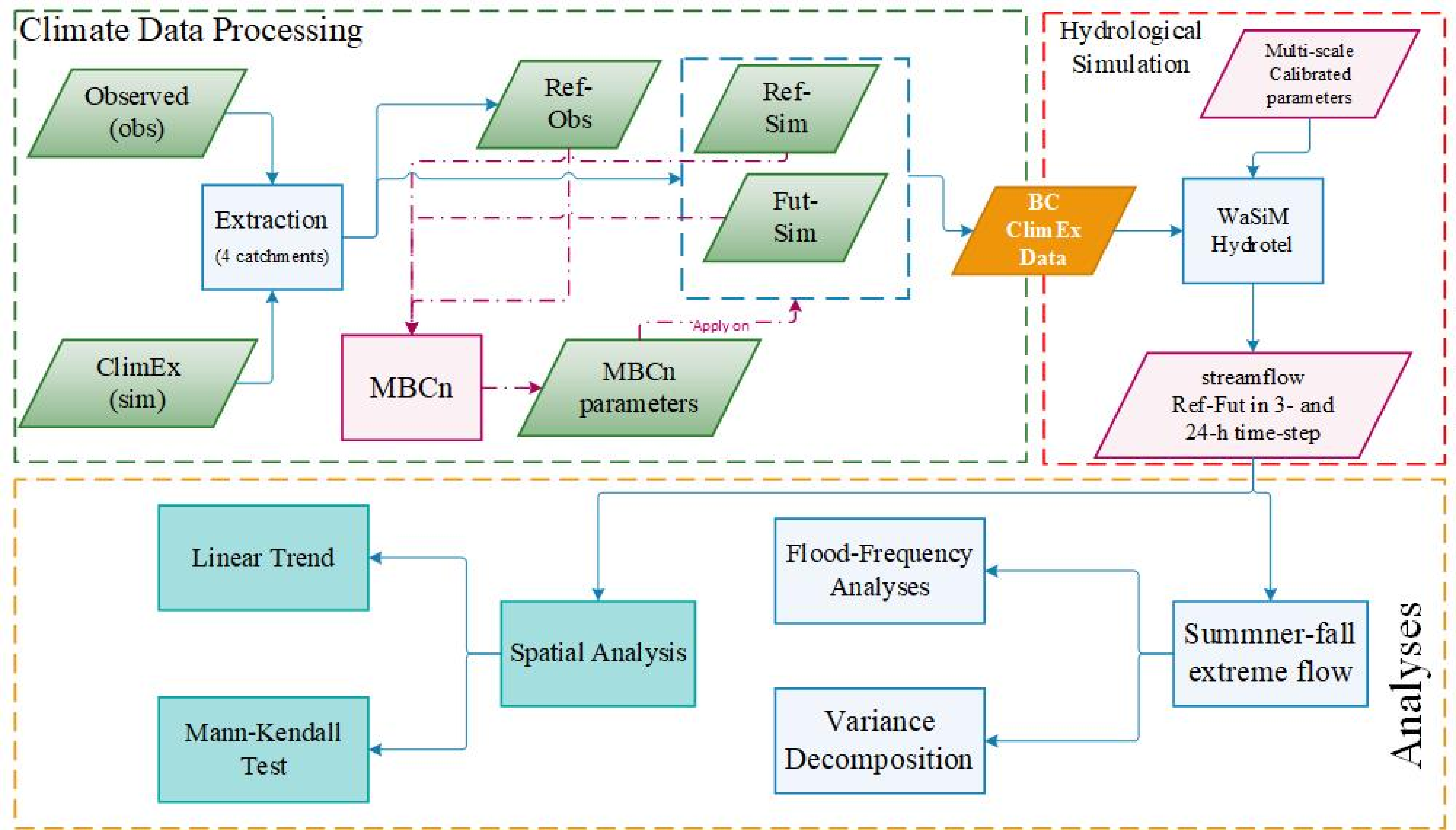

Climate Data Processing
Observed (obs)
ClimEx (sim)
Extraction (4 catchments)
Ref-Obs
Ref-Sim
Fut-Sim
MBCn
MBCn parameters
Apply on
BC ClimEx Data
Hydrological Simulation
Multi-scale Calibrated parameters
WaSiM Hydrotel
streamflow Ref-Fut in 3- and 24-h time-step
Analyses
Linear Trend
Mann-Kendall Test
Spatial Analysis
Flood-Frequency Analyses
Variance Decomposition
Summner-fall extreme flow

**Figure 2.**

75° N
60° N
45° N
135° W
120° W
105° W
90° W
75° W
60° W
Croche
Boyer
Aux Brochets
Chaudière
48°N
47°N
46°N
45°N
Latitude
74°W
72°W
70°W
Longitude
50 km
50 mi

**Figure 3.**

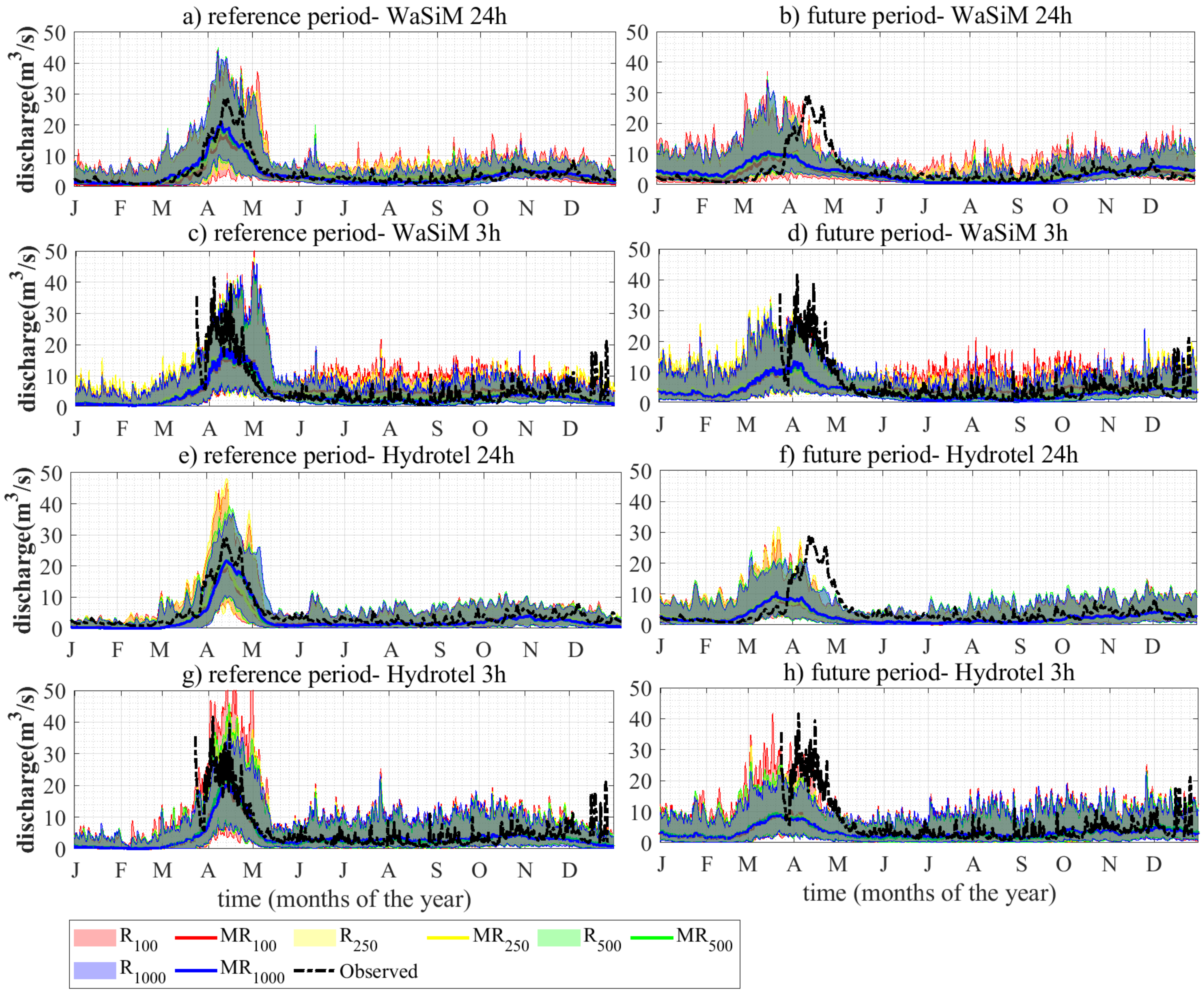

a) reference period- WaSiM 24h
b) future period- WaSiM 24h
c) reference period- WaSiM 3h
d) future period- WaSiM 3h
e) reference period- Hydrotel 24h
f) future period- Hydrotel 24h
g) reference period- Hydrotel 3h
h) future period- Hydrotel 3h
discharge(m3/s)
0 10 20 30 40 50
J F M A M J J A S O N D
time (months of the year)
R100 MR100 R250 MR250 R500 MR500
R1000 MR1000 Observed

**Figure 4.**

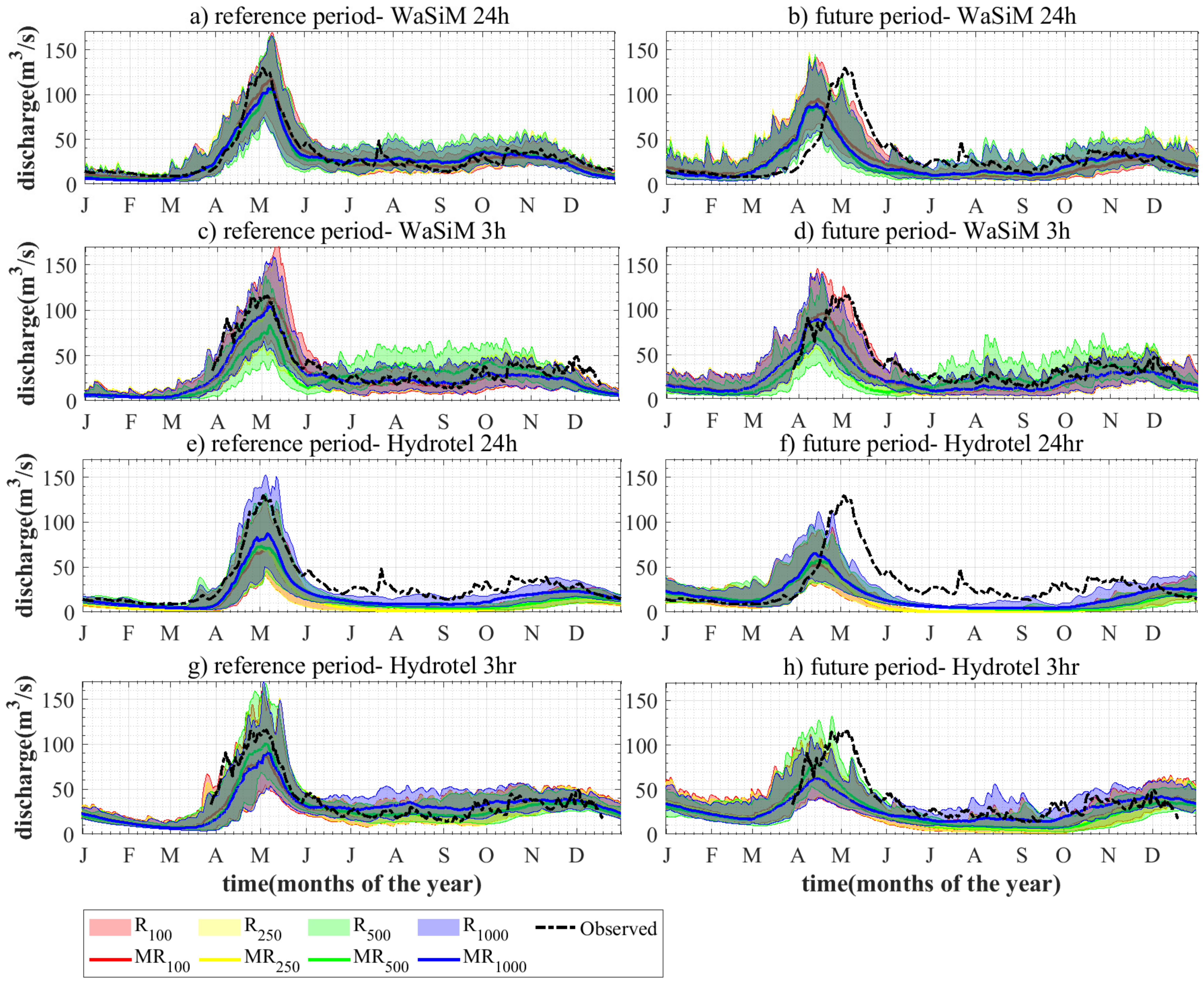

a) reference period- WaSiM 24h
b) future period- WaSiM 24h
c) reference period- WaSiM 3h
d) future period- WaSiM 3h
e) reference period- Hydrotel 24h
f) future period- Hydrotel 24hr
g) reference period- Hydrotel 3hr
h) future period- Hydrotel 3hr
discharge(m3/s)
0
50
100
150
J F M A M J J A S O N D
time(months of the year)
R100
R250
R500
R1000
Observed
MR100
MR250
MR500
MR1000

**Figure 5.**

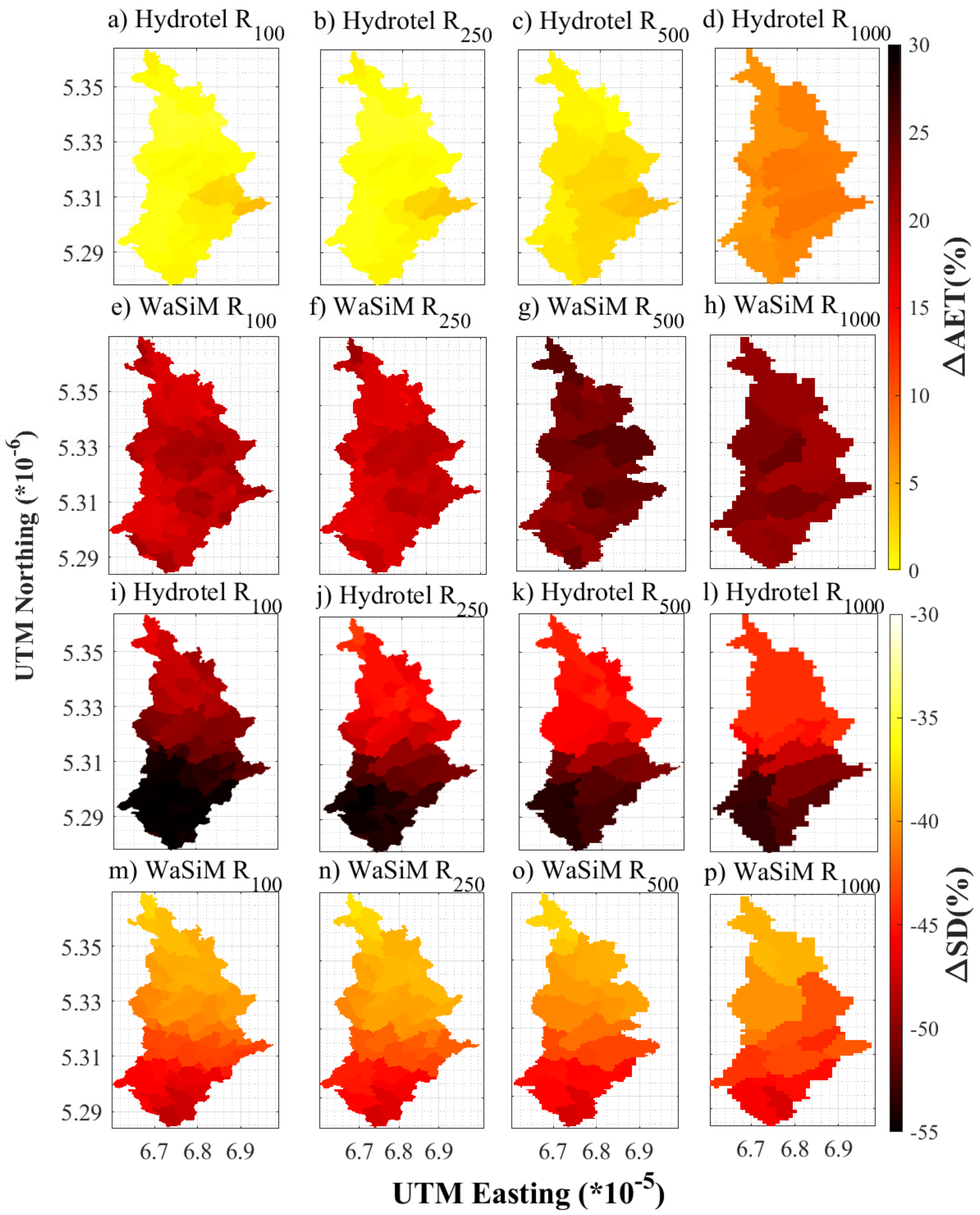

a) Hydrotel R100
b) Hydrotel R250
c) Hydrotel R500
d) Hydrotel R1000
e) WaSiM R100
f) WaSiM R250
g) WaSiM R500
h) WaSiM R1000
i) Hydrotel R100
j) Hydrotel R250
k) Hydrotel R500
l) Hydrotel R1000
m) WaSiM R100
n) WaSiM R250
o) WaSiM R500
p) WaSiM R1000
ΔAET(%)
30
25
20
15
10
5
0
ΔSD(%)
-30
-35
-40
-45
-50
-55
5.35
5.33
5.31
5.29
6.7 6.8 6.9
UTM Northing (*10^-6)
UTM Easting (*10^-5)

**Figure 6.**

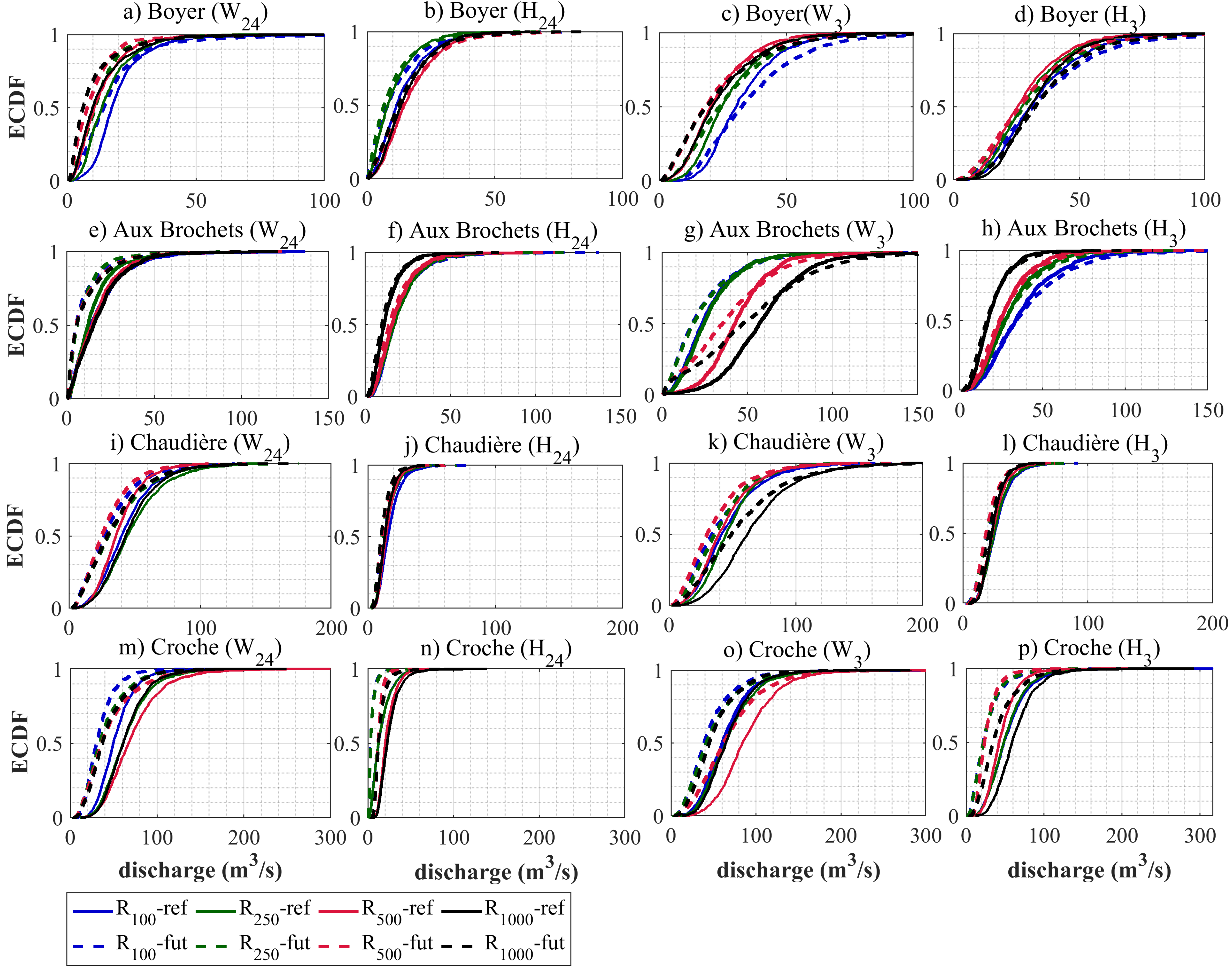

a) Boyer ($W_{24}$)
b) Boyer ($H_{24}$)
c) Boyer($W_3$)
d) Boyer ($H_3$)
e) Aux Brochets ($W_{24}$)
f) Aux Brochets ($H_{24}$)
g) Aux Brochets ($W_3$)
h) Aux Brochets ($H_3$)
i) Chaudière ($W_{24}$)
j) Chaudière ($H_{24}$)
k) Chaudière ($W_3$)
l) Chaudière ($H_3$)
m) Croche ($W_{24}$)
n) Croche ($H_{24}$)
o) Croche ($W_3$)
p) Croche ($H_3$)
ECDF
discharge ($m^3/s$)
$R_{100}$-ref
$R_{250}$-ref
$R_{500}$-ref
$R_{1000}$-ref
$R_{100}$-fut
$R_{250}$-fut
$R_{500}$-fut
$R_{1000}$-fut

**Figure 7.**

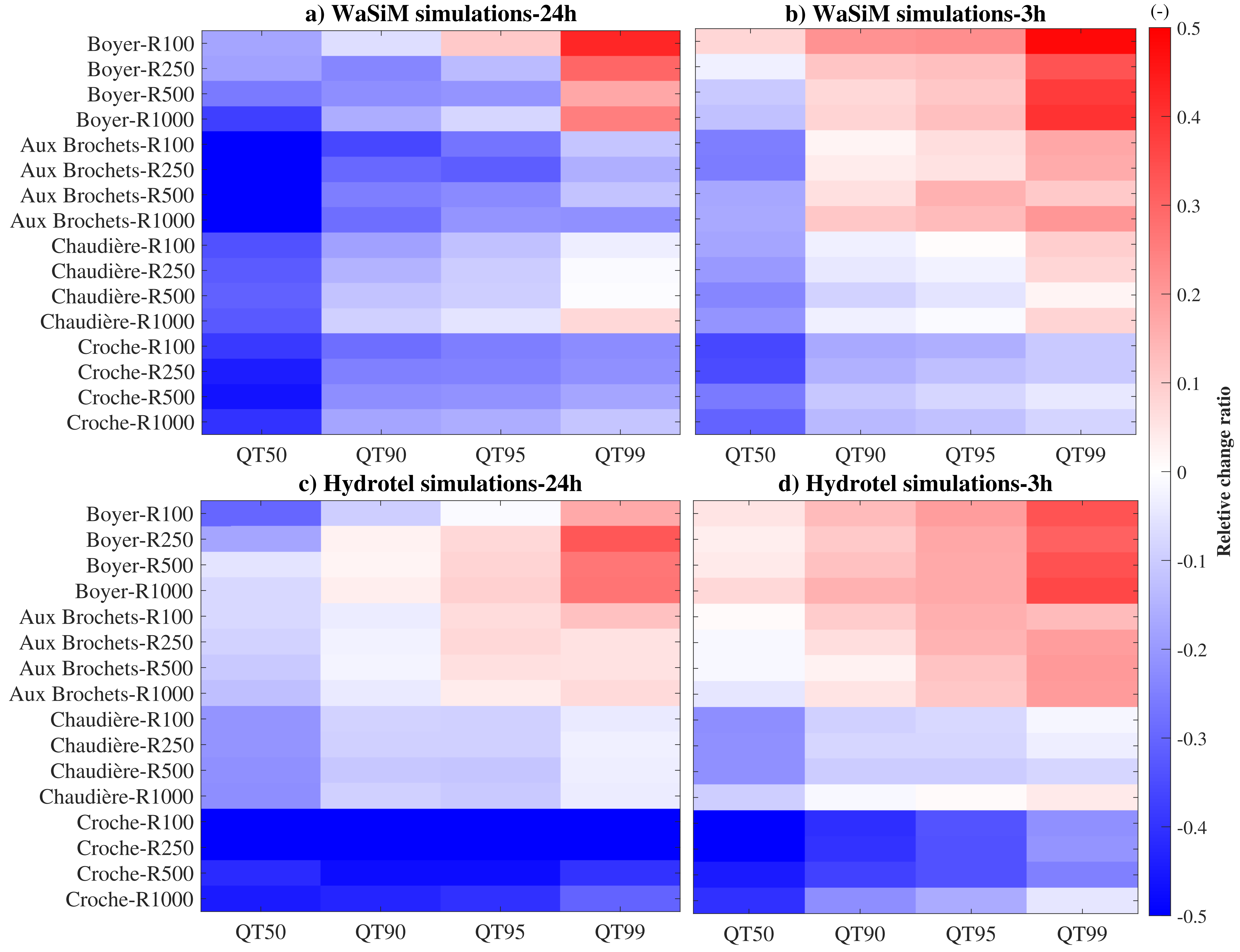

a) WaSiM simulations-24h
b) WaSiM simulations-3h
c) Hydrotel simulations-24h
d) Hydrotel simulations-3h
Boyer-R100
Boyer-R250
Boyer-R500
Boyer-R1000
Aux Brochets-R100
Aux Brochets-R250
Aux Brochets-R500
Aux Brochets-R1000
Chaudière-R100
Chaudière-R250
Chaudière-R500
Chaudière-R1000
Croche-R100
Croche-R250
Croche-R500
Croche-R1000
QT50
QT90
QT95
QT99
(-)
0.5
0.4
0.3
0.2
0.1
0
-0.1
-0.2
-0.3
-0.4
-0.5
Reletive change ratio

**Figure 8.**

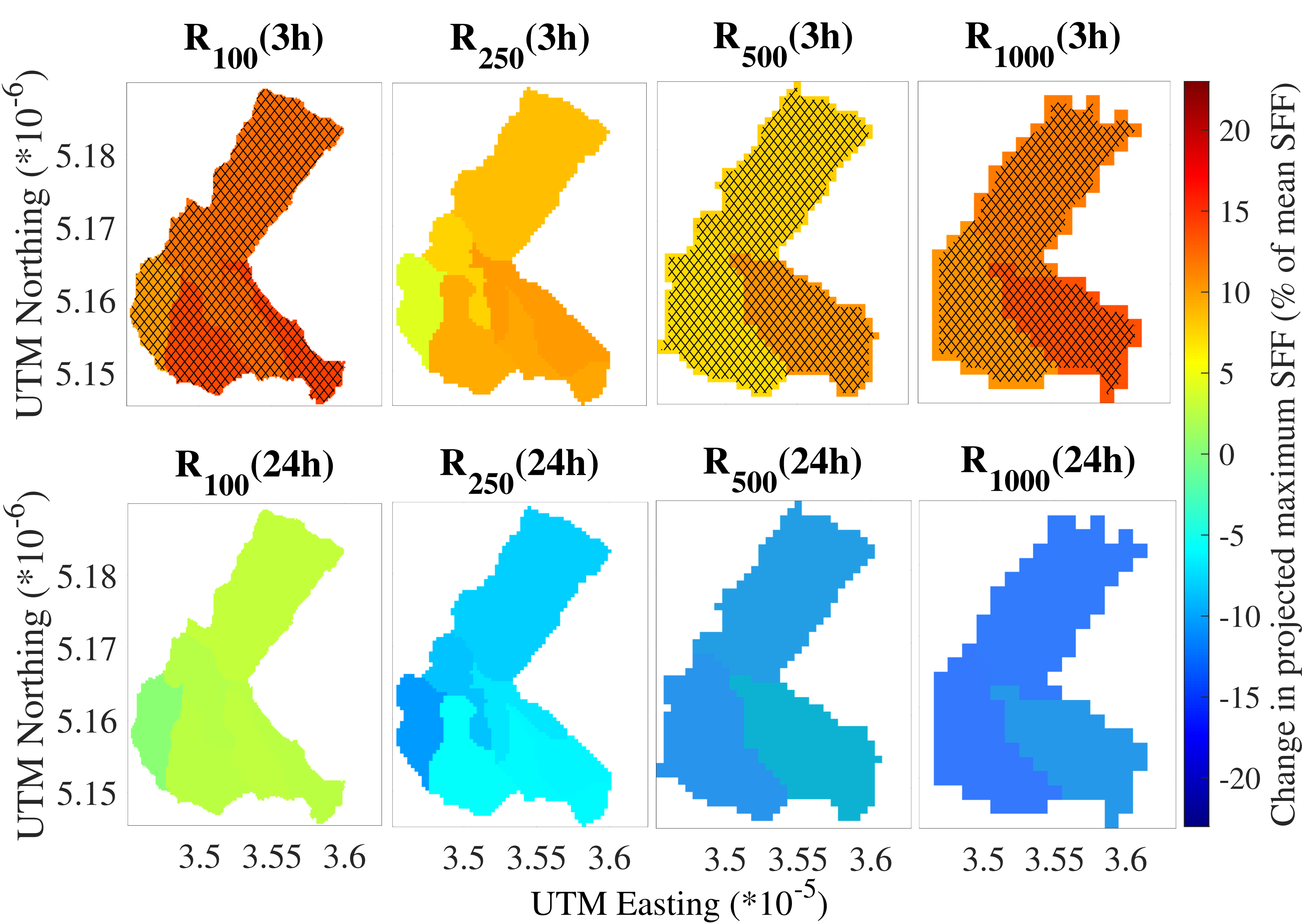

R100(3h)
R250(3h)
R500(3h)
R1000(3h)
R100(24h)
R250(24h)
R500(24h)
R1000(24h)
UTM Northing (*10^-6)
5.18
5.17
5.16
5.15
UTM Easting (*10^-5)
3.5
3.55
3.6
Change in projected maximum SFF (% of mean SFF)
20
15
10
5
0
-5
-10
-15
-20

**Figure 9.**

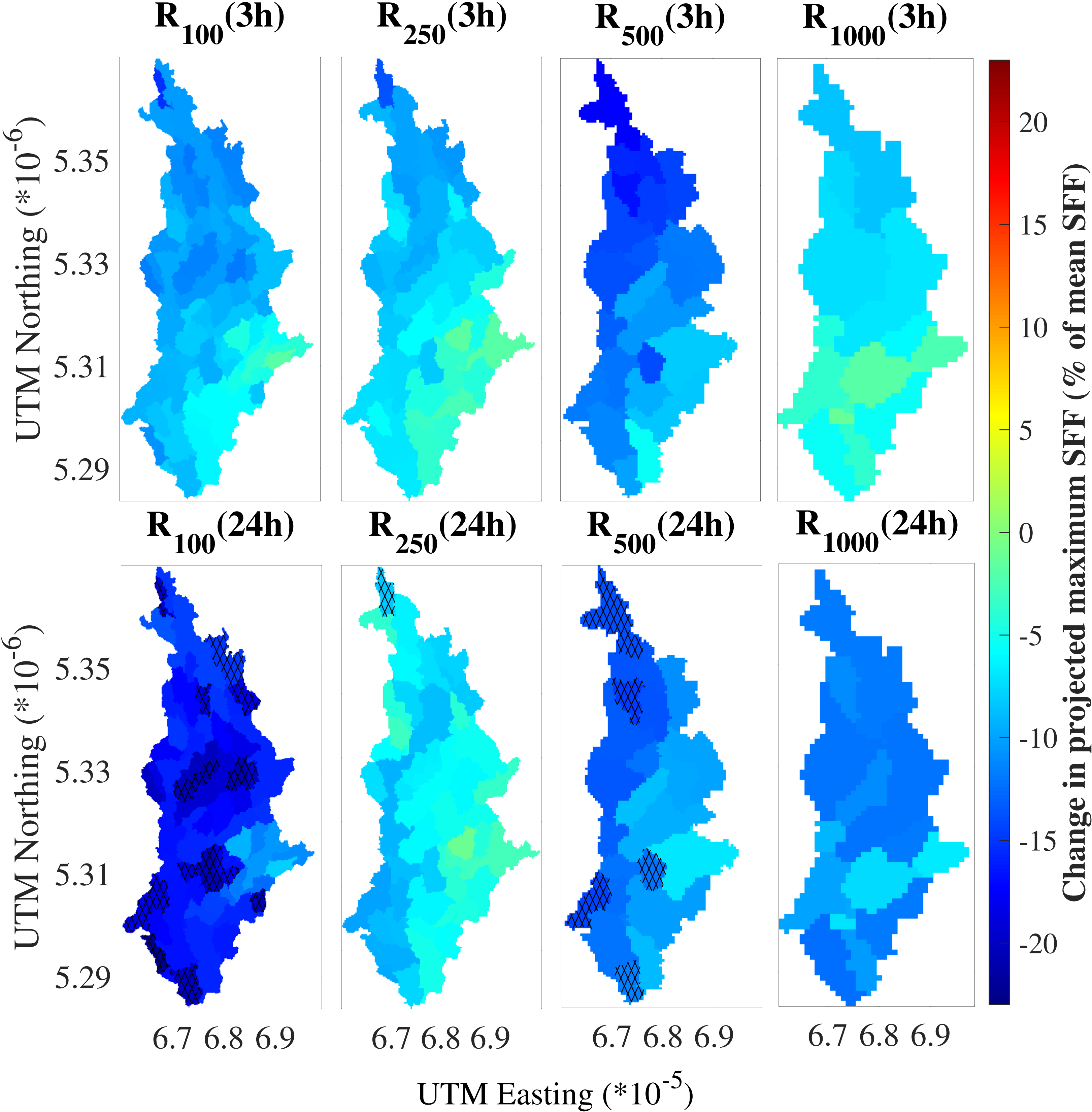

R100(3h)
R250(3h)
R500(3h)
R1000(3h)
R100(24h)
R250(24h)
R500(24h)
R1000(24h)
UTM Northing (*10^-6)
5.35
5.33
5.31
5.29
UTM Easting (*10^-5)
6.7 6.8 6.9
Change in projected maximum SFF (% of mean SFF)
20
15
10
5
0
-5
-10
-15
-20

**Figure 10.**

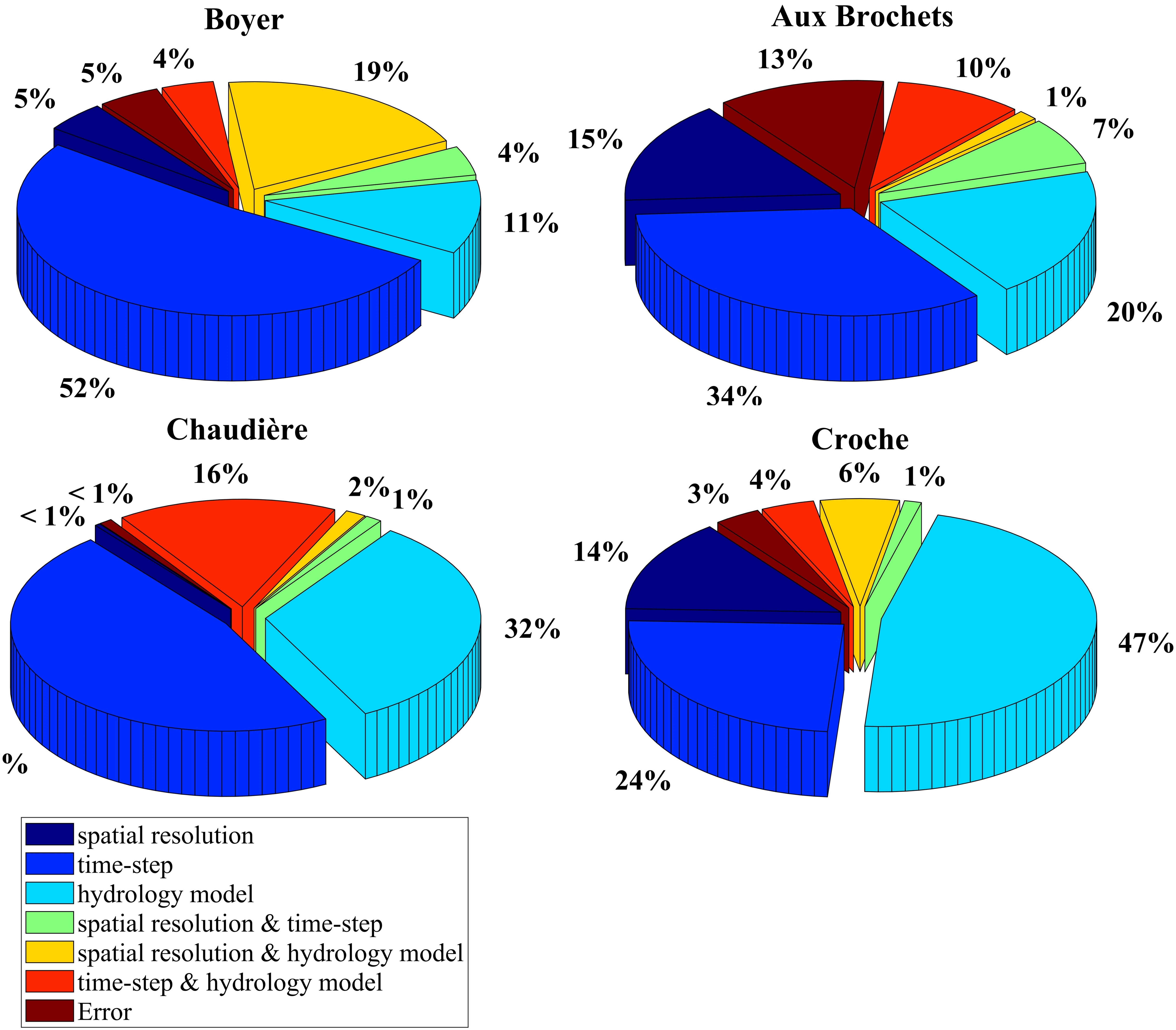

Boyer
5%
5%
4%
19%
4%
11%
52%
Aux Brochets
13%
10%
1%
7%
15%
20%
34%
Chaudière
< 1%
< 1%
16%
2%
1%
32%
47%
Croche
3%
4%
6%
1%
14%
47%
24%
spatial resolution
time-step
hydrology model
spatial resolution & time-step
spatial resolution & hydrology model
time-step & hydrology model
Error